Concept Paper

A Theranostic Implant Platform for In Vivo Infection Monitoring and Light-Based Therapy

Christoph Dillitzer *, Muammer Can Sezgin, Nguyen Bach Tran, Paul Morandell, Vincent Lallinger, Igor Lazic, Oliver Hayden, Rainer Burgkart

Posted Date: 27 April 2026

doi: 10.20944/preprints202604.1875.v1

Keywords: theranostic implant; smart spacer; periprosthetic joint infection; light-based therapy; biofilm; in vivo monitoring

 doi:10.20944/preprints202604.1875.v1

Concept Paper

A Theranostic Implant Platform for In Vivo Infection Monitoring and Light-Based Therapy

Christoph Dillitzer [1,*], Muammer Can Sezgin [1], Nguyen Bach Tran [1], Paul Morandell [1], Vincent Lallinger [2], Igor Lazic [2], Oliver Hayden [1] and Rainer Burgkart [2]

[1] School of Computation, Information and Technology, Technical University of Munich, Munich, Germany

[2] Department of Orthopedics, Technical University of Munich, Munich, Germany

* Correspondence: christoph.dillitzer@tum.de

Abstract

Periprosthetic joint infection (PJI) remains a major limitation of joint arthroplasty, driven by the absence of localized, continuous diagnostics and controllable in vivo therapy during the spacer interval. Here, we introduce a theranostic implant platform that integrates sensing, communication, and light-based intervention within a temporary joint spacer. The SmartSpacer enables real-time intra-articular monitoring, combining high-resolution temperature sensing (± 0.1 °C), optical imaging, and spectral detection of bacterial activity down to ~10^3 CFU ml^{-1}. We establish a translation-oriented framework that maps wavelength-dependent antimicrobial effects onto implant-level constraints. Within this framework, visible blue light provides continuous suppression of bacterial growth, while ultraviolet radiation enables rapid bactericidal action via pulsed, spatially confined exposure. These modalities operate within implant-compatible energy budgets and without measurable thermal load, enabling sustained and repeatable intervention. Continuous multimodal sensing enables longitudinal tracking of infection dynamics, transforming diagnostics from static assessment to predictive monitoring. By linking localized sensing with controllable therapy, the SmartSpacer converts the spacer interval from a passive waiting phase into an active treatment window. This work defines a system-level strategy for implant-based infection control and establishes a foundation for future feedback-driven, closed-loop therapeutic systems.

Keywords: theranostic implant; smart spacer; periprosthetic joint infection; light-based therapy; biofilm; in vivo monitoring

1. Introduction

1.1. The Unresolved Clinical Challenge of Periprosthetic Joint Infection

Periprosthetic joint infection (PJI) remains one of the most severe complications in modern orthopedic surgery, posing a substantial clinical and economic burden on healthcare systems worldwide.[1–3] The growing demand for joint replacements, already reaching several hundred thousand knee arthroplasties annually in the United States, is projected to exceed one million procedures per year in the coming decades.[4,5] This rise is driven by a rapidly ageing population, with the proportion of individuals aged ≥65 years set to increase markedly by 2050, fundamentally reshaping the clinical landscape of joint replacement[6,7]. Total knee arthroplasty (TKA) is routinely performed to treat advanced joint degeneration and inflammatory conditions. Despite continuous advancements in implant design, surgical techniques, and perioperative management, infection remains a clinically relevant complication. Primary infection rates are typically 1–2%, but given the rapidly increasing number of procedures, the absolute burden is substantial. Following revision surgeries, infection rates increase dramatically and can exceed 30%, with each additional surgical intervention further compounding patient risk and system complexity.[8–10]

 doi:10.20944/preprints202604.1875.v1

The current gold standard for treating chronic PJI is the two-stage revision procedure.[11,12] This involves removal of the infected implant, extensive debridement, and implantation of an antibiotic-loaded spacer.[13] After this first stage, bacteria frequently persist within the joint environment, particularly in protected niches and biofilm structures on residual tissue or implant surfaces. During the spacer interval, antimicrobial treatment relies primarily on antibiotic diffusion from polymethyl methacrylate (PMMA) and systemic therapy.[14] However, due to material-related release kinetics, local antibiotic concentrations decline, typically within the first 2 days, depending on material and doses, while the spacer remains implanted for several weeks, commonly 2–6 weeks and in some cases up to 3 months. Importantly, the presence of a spacer does not imply eradication of infection. Persistent intra-articular bacteria may survive and potentially recolonize the joint environment. In a significant number of cases, additional spacer exchanges are required, further increasing surgical burden and patient morbidity.[15–17]

A central challenge arises at the transition between spacer implantation and re-implantation of the definitive prosthesis.[18,19] The decision on the timing of re-implantation is currently based largely on the surgeon's subjective assessment, supported by indirect clinical parameters such as systemic inflammatory markers, patient symptoms, and limited microbiological sampling.[20–23] Objective, localized, and continuous information about the infection status within the joint is not available. This lack of reliable intra-articular data introduces a critical uncertainty into the treatment pathway (Figure 1). Premature re-implantation may result in persistent infection and early failure, whereas delayed intervention prolongs patient immobility, increases complication risk, and leads to substantial additional healthcare costs.[24,25] PJIs are not only a local complication but a condition with profound systemic consequences. Mortality following revision surgery for infection is markedly higher than for aseptic failure, reaching 11% versus 2.0% up to 26% versus 13% at five years. Even after adjustment for demographic factors and comorbidities, infection remains an independent predictor of death, conferring an approximately fivefold increased mortality risk[26]. Taken together, current treatment strategies are fundamentally constrained by two critical limitations:

- Lack of continuous, localized infection diagnostics, and
- Absence of active, controllable in vivo therapeutic interventions within the joint space.

These limitations define a clear and urgent clinical unmet need: the ability to monitor and actively modulate the intra-articular infection state during the spacer interval, thereby enabling evidence-based decision-making and improved treatment outcomes[27].

 doi:10.20944/preprints202604.1875.v1

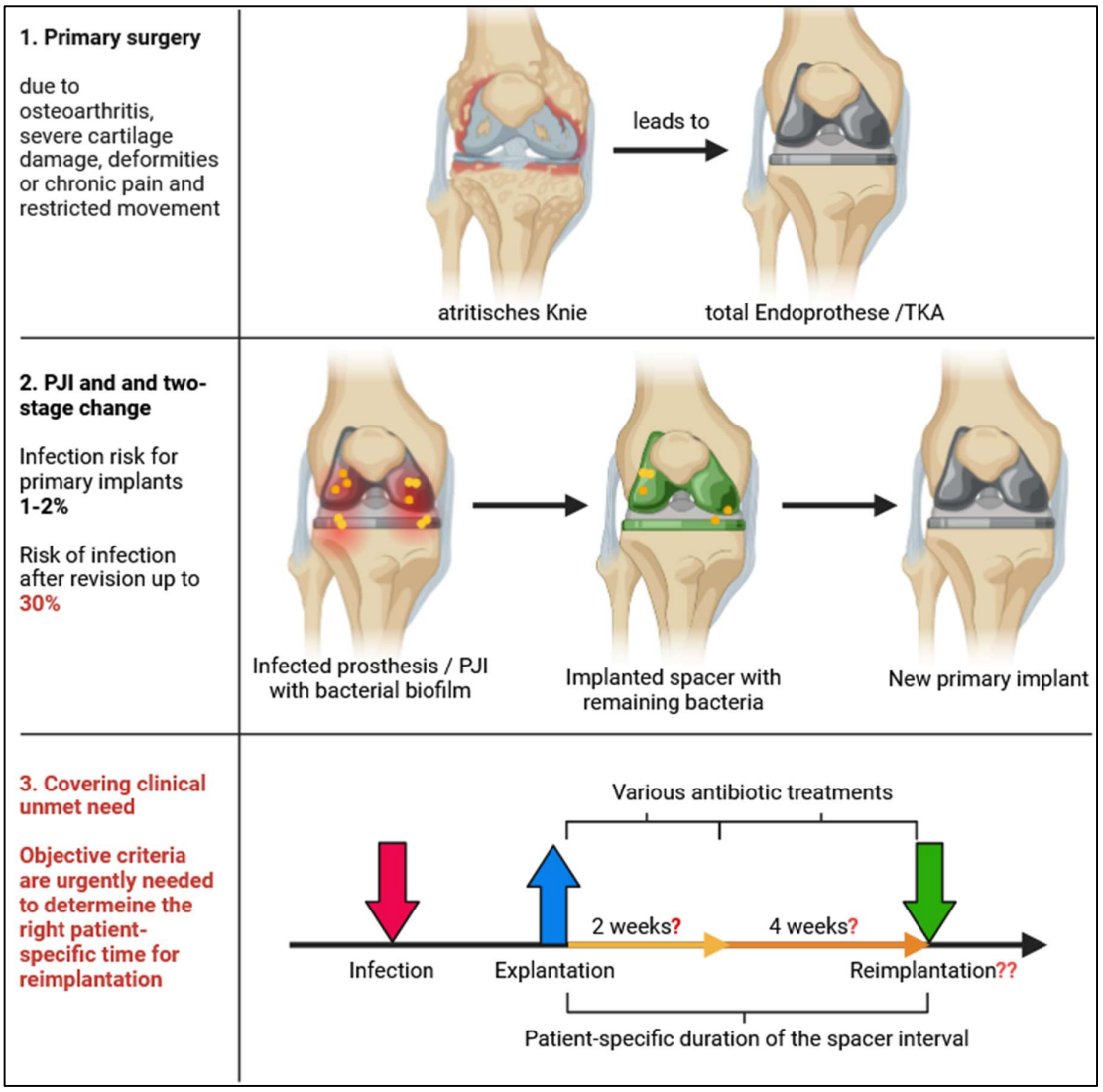

Figure 1. Clinical workflow and decision gap in two-stage revision for periprosthetic joint infection. (1) Primary total knee arthroplasty (TKA). (2) Infection onset and two-stage revision with spacer implantation, where residual bacteria may persist despite debridement and antibiotic release. (3) Spacer interval lacking objective, localized infection monitoring, resulting in uncertainty in re-implantation timing and risk of suboptimal clinical decisions.

1.2. Failure of the Current Treatment Paradigm

The limitations of the two-stage revision approach are not merely technological but conceptual. The current paradigm treats infection primarily through surgical intervention and antibiotic administration, while the spacer itself remains a passive component with limited therapeutic functionality.

During the spacer interval, residual microorganisms can persist in the joint environment despite aggressive debridement. These pathogens may reside in biofilms, microscopic cavities, or poorly perfused tissue regions, rendering them difficult to eliminate by antibiotics alone[3,28]. Crucially, the duration of effective antibiotic activity is short compared to the total implantation time. While spacers remain in situ for weeks to months, antibiotic diffusion from PMMA effectively decreases after ~2 days, resulting in a prolonged period of sub-therapeutic exposure.[16,17] At the same time, there is no method available today that allows clinicians to directly assess the local infection state in vivo over time. The absence of real-time, spatially resolved diagnostics results in a “blind interval” between

 doi:10.20944/preprints202604.1875.v1

explantation and re-implantation. In addition, current therapeutic strategies are largely static. Antibiotic-loaded spacers provide an initial burst release but do not allow dynamic adjustment of treatment based on the evolving infection status. Consequently, therapy cannot be personalized, modulated, or actively controlled in response to the local biological environment. This paradigm, characterized by passive implants, indirect diagnostics, and non-adaptive therapy, is increasingly insufficient to address the complexity of PJI, particularly in the context of rising antimicrobial resistance.

1.3. Light-Based Therapies as a Missing Link for In Vivo Infection Control

Electromagnetic (EM) radiation is deeply embedded in modern medicine, spanning both diagnostic and therapeutic domains. Imaging modalities such as magnetic resonance imaging (MRI), computed tomography (CT), and positron emission tomography (PET) rely on controlled EM interactions to generate high-resolution representations of internal structures. In parallel, a wide spectrum of therapeutic approaches, including laser surgery, photodynamic therapy (PDT), ultraviolet (UV) irradiation, and low-level light therapy (LLLT), demonstrates that targeted EM exposure can actively modulate biological processes and treat disease.[29]

Across multiple clinical disciplines, light-based therapies have reached a high level of maturity. In dermatology, UV and visible light are routinely applied for inflammatory and infectious conditions. In dentistry, optical radiation is used for both antimicrobial treatment and tissue regeneration. Ophthalmology, neonatal care (e.g., jaundice treatment), and even neuropsychiatric applications such as light therapy for depressive disorders further illustrate the broad clinical relevance of photonic interventions. In addition, phototherapeutic and photodiagnostic techniques have become increasingly important in oncology and wound healing, enabling spatially and temporally controlled interventions.[30–34]

At the same time, a growing body of preclinical and clinical research demonstrates the effectiveness of light-based strategies against some of the most challenging medical problems, including multidrug-resistant pathogens, epithelial carcinomas, and biofilm-associated infections on implant surfaces. These developments highlight not only the antimicrobial potential of EM radiation but also its capacity to interact with complex biological systems in a controlled and tunable manner.[35,36]

Despite this extensive and rapidly evolving landscape, one critical gap remains: the application of localized, in vivo light-based therapy for the treatment of periprosthetic joint infections. This absence is particularly striking when viewed in the context of total endoprosthesis surgery, (Figure 2) where the clinical demand for effective infection control strategies is exceptionally high and where conventional approaches are often limited.

The underlying reason for this gap has historically been technological. Delivering controlled radiation to a confined anatomical space such as a joint cavity has not been feasible due to the lack of suitable implantable platforms, insufficient miniaturization of light sources, and challenges related to energy delivery and thermal management. As a result, light-based antimicrobial strategies have largely remained restricted to external or minimally invasive applications.

Recent advances fundamentally change this situation. The convergence of miniaturized optoelectronic components, energy-efficient light-emitting diodes (LEDs), and integrated sensing technologies now enables the incorporation of optical functionality directly into implantable medical devices. Within this context, temporary joint spacers provide a uniquely suitable platform: their established clinical use, combined with the optical properties of materials such as polymethyl methacrylate (PMMA), allows direct interaction between embedded light sources and the surrounding tissue environment without additional invasive delivery pathways.

Furthermore, the inherently limited implantation period, typically spanning several weeks, defines a controlled therapeutic window in which localized interventions can be applied under manageable safety constraints. This temporal confinement aligns well with the requirements of dose-controlled phototherapy and facilitates risk mitigation.

 doi:10.20944/preprints202604.1875.v1

Taken together, these developments bridge previously disconnected domains: clinical requirements for infection control in joint arthroplasty, established light-based therapies across multiple medical disciplines, and emerging research targeting resistant pathogens and biofilm-associated infections. This convergence enables, for the first time, a new therapeutic paradigm:

Localized, controllable, and repeatable in vivo light-based therapy directly within the joint space.

This paradigm forms the conceptual foundation for theranostic implant systems that integrate continuous monitoring with active, light-mediated intervention, thereby redefining the role of temporary implants in infection management.

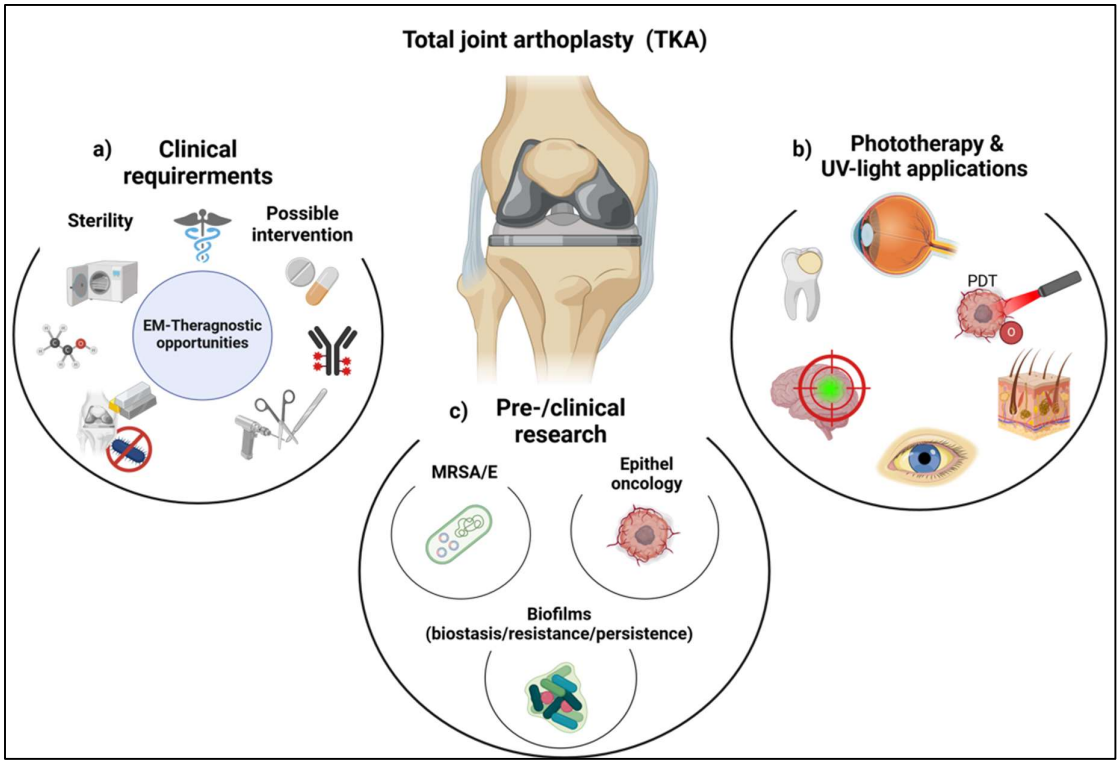

Figure 2. Convergence of clinical need, mature photonic therapies, and emerging antimicrobial research as the foundation for implant-based light intervention. a) Infection control requirements in joint arthroplasty. b) Established clinical use of light-based therapies. c) Emerging strategies targeting biofilms and resistant pathogens.

2. Concept of a Theranostic Implant System

To overcome the fundamental limitations of current treatment strategies, a conceptual shift from passive implants toward theranostic systems is required. Such systems integrate diagnostic and therapeutic functionalities within a single device and enable direct interaction with the local biological environment.

In contrast to conventional spacers, which primarily serve a mechanical and drug-delivery function, a theranostic implant establishes a closed-loop approach to infection management. This approach is based on three interconnected capabilities: continuous sensing of relevant physiological and biochemical parameters, real-time interpretation of the local infection state, and targeted therapeutic intervention directly at the site of interest.

By linking these elements, theranostic systems enable dynamic adaptation of treatment strategies based on objective data rather than indirect clinical surrogates. In the specific context of PJI, this approach has the potential to fundamentally transform the spacer interval, from a passive waiting period into an active, controllable treatment phase.

 doi:10.20944/preprints202604.1875.v1

2.1. The SmartSpacer Platform Architecture

The SmartSpacer represents a platform technology that extends conventional antibiotic-loaded spacers into multifunctional theranostic implant systems. Building upon established polymethyl methacrylate (PMMA)-based designs, the platform integrates miniaturized optoelectronic components directly within the implant structure, enabling localized sensing, therapeutic actuation, and wireless communication within a single device.

At its core, the system enables continuous acquisition of clinically relevant intra-articular biomarkers. High-resolution temperature sensing (±0.1 °C) provides a sensitive measure of local inflammatory dynamics, while integrated optical imaging allows direct visualization of infection-associated morphological changes, including vascularization, turbidity, and tissue alterations. Complementing these modalities, miniaturized spectral sensing enables the detection of bacterial presence and metabolic activity, with experimentally demonstrated sensitivities down to approximately 10^3 CFU ml^{-1}. Together, these signals provide a direct, localized representation of the infection state within the joint environment, overcoming the limitations of systemic surrogate markers.[37]

Importantly, diagnostic relevance arises not from isolated measurements but from longitudinal trend analysis. Continuous monitoring over time enables the identification of stable physiological baselines as well as subtle deviations, such as gradual temperature increases or progressive spectral shifts, which may indicate early-stage reinfection before clinical manifestation. This temporal dimension transforms sensing from a descriptive tool into a predictive diagnostic framework.

In parallel to sensing, the SmartSpacer incorporates embedded light sources that enable localized electromagnetic therapy directly at the implant–tissue interface. These therapeutic functionalities are supported by integrated electronics for signal processing and control, as well as wireless communication interfaces that allow real-time data access and external system interaction. The resulting architecture establishes the foundation for a closed-loop system in which diagnostic information and therapeutic intervention are intrinsically linked. All relevant parameters are continuously tracked over time, enabling comprehensive longitudinal monitoring of the local physiological and pathological state. Importantly, this data-driven framework does not operate autonomously but remains under full clinical control: physicians retain continuous oversight and can actively decide if, when, and how therapeutic interventions are applied, ensuring safe, transparent, and patient-specific treatment adaptation. A dedicated energy management concept ensures operation under the strict constraints of an implantable system, balancing limited power availability with sensing, communication, and therapeutic performance. Depending on the LED configuration, optical power levels of up to ~5 mW can be delivered at the implant–tissue interface, defining the available energy budget for localized therapy. The currently integrated LEDs are primarily utilized for illumination of the camera system and for spectroscopic measurements. However, the platform design inherently provides multiple additional integration sites, enabling the incorporation of dedicated LEDs with application-specific wavelengths for therapeutic purposes.

Initial experimental observations indicate measurable bacterial inhibition at low energy densities under implant-relevant conditions, demonstrating compatibility between antimicrobial efficacy and system-level constraints. Due to pulsed operation, no cumulative thermal buildup is observed, ensuring stable operation within physiological limits.

Thermal characterization therefore reflects not only peak power dissipation but also the temporal structure of operation, enabling repeated therapeutic intervention without measurable temperature increase. In parallel, longitudinal signal analysis enables detection of infection-related changes at bacterial concentrations on the order of ~10^3 CFU ml^{-1}, providing a direct link between sensing sensitivity and clinically relevant infection thresholds. Together, these parameters define a bounded operational regime in which sensing, therapy, and system stability can be jointly realized within an implantable platform. (Figure 3; Table 1).[38–40]

The development of the SmartSpacer platform is supported by a multi-year research program funded by the German Federal Ministry of Education and Research, reflecting both its technological

 doi:10.20944/preprints202604.1875.v1

maturity and clinical relevance. Over the course of this program, the system has progressed from early prototypical concepts to an integrated implantable platform. At the current stage, the technology is undergoing preclinical validation in a large-animal model, where initial results indicate that core functionalities, including sensing, communication, and structural integration, can be reliably achieved under physiologically relevant conditions, supporting the feasibility of the approach and its potential for clinical translation.[41]

The diagnostic capability of the SmartSpacer is defined by the integration of complementary detector modalities, each targeting distinct yet interrelated biomarker classes within the intra-articular environment. Rather than relying on isolated measurements, the system establishes a multimodal sensing framework that captures inflammatory, structural, and microbial signatures in a spatially co-localized and temporally resolved manner. Temperature sensing provides a direct and highly sensitive measure of local inflammatory dynamics. Subtle deviations from physiological baseline levels reflect changes in perfusion, immune activity, and infection progression, enabling early detection of pathological processes. In addition, physiological temperature regulation follows a circadian rhythm characterized by predictable diurnal fluctuations. In the context of periprosthetic joint infection, this pattern is frequently disrupted, with local temperature elevations accompanied by a loss or attenuation of circadian variability. Such deviations from the normal temporal profile provide an additional, highly sensitive indicator of inflammatory activity and may further enhance early detection capabilities.[42]

Optical imaging extends this capability by resolving morphological and structural biomarkers in situ. Changes in tissue appearance, including increased turbidity, altered vascularization patterns, and surface irregularities, serve as visual indicators of infection-associated remodeling within the joint cavity.[43–46]

Complementing these modalities, spectral sensing enables access to functional microbial biomarkers. Wavelength-dependent absorption and scattering signatures reflect bacterial presence, concentration, and metabolic activity, allowing detection of infection-related changes. These spectral features originate from endogenous chromophores and structural components, providing a label-free approach to microbial characterization.

Crucially, the diagnostic value of these signals emerges from their longitudinal integration. The SmartSpacer does not interpret biomarkers as static endpoints, but as dynamic trajectories. Temporal correlations between temperature evolution, morphological alterations, and spectral shifts enable differentiation between transient physiological variation and persistent pathological change. This transforms sensing into a predictive framework, capable of identifying early-stage reinfection and guiding therapeutic intervention.

The resulting architecture establishes the foundation for a closed-loop system in which diagnostic information and therapeutic intervention are intrinsically linked. While full closed-loop control is not yet implemented, the presented system establishes the necessary integration of sensing and actuation required for future feedback-driven therapeutic strategies.

 doi:10.20944/preprints202604.1875.v1

Table 1. Multimodal detector–biomarker mapping within the SmartSpacer system.[37].

Detector modality	Measured signal	Biomarker class	Biological interpretation	Diagnostic role
Temperature sensor	Local temperature	Inflammatory biomarker	Local immune response, perfusion changes, infection onset	Early detection, trend monitoring
Optical imaging (camera)	Tissue morphology, turbidity, structure	Structural / morphological	Vascularization, biofilm presence, tissue alteration	Spatial assessment of infection environment
Spectral sensor	Absorption / scattering signatures	Microbial / metabolic	Bacterial load, metabolic activity, chromophore response	Quantification of infection state
Multimodal integration	Temporal signal correlation	Dynamic biomarker (trend)	Evolution of infection vs. physiological baseline	Predictive diagnostics, therapy guidance

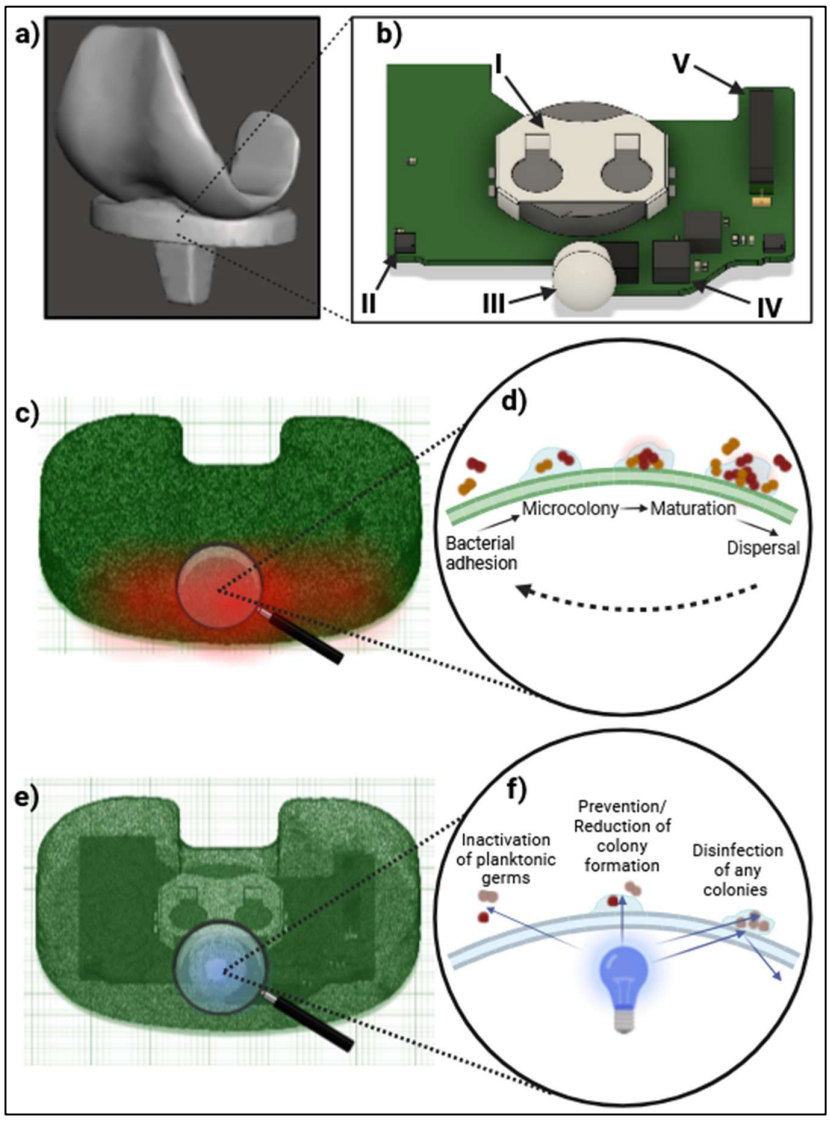

Figure 3. Transition from passive spacer to theranostic SmartSpacer enabling localized sensing and light-based intervention. a) Conventional spacer. b) Integrated sensor architecture. c)&d) Bacterial persistence and biofilm dynamics. e) SmartSpacer with optical interface. f) Controlled, localized antimicrobial light application.

 doi:10.20944/preprints202604.1875.v1

2.2. Optical Accessibility as a Unique Advantage

A defining feature of the SmartSpacer platform is its inherent optical accessibility, enabled by the use of transparent or semi-transparent polymethyl methacrylate (PMMA) regions integrated into the implant structure. This property establishes a direct optical interface between embedded optoelectronic components and the surrounding biological environment, representing a fundamental distinction from conventional implant systems and external light-delivery approaches.

In contrast to fiber-based or transcutaneous illumination strategies, which are limited by strong attenuation, scattering losses, and restricted spatial control, the SmartSpacer enables localized emission and detection directly within the joint cavity. This configuration minimizes optical path length and reduces energy loss, allowing efficient coupling of both sensing and therapeutic signals to the target tissue. As a result, optical measurements, such as imaging and spectral analysis, can be performed with improved signal fidelity, while therapeutic irradiation can be applied with higher spatial precision and reduced off-target exposure.

The intra-articular environment further amplifies this advantage. As a confined and optically bounded space, the joint cavity enables controlled light propagation and spatial confinement, improving measurement stability and establishing a predictable relationship between delivered energy and biological response. Optical accessibility thus becomes a key enabler for reliable biomarker acquisition and controlled therapeutic dosing.

From a diagnostic perspective, the direct optical interface enables continuous, non-invasive monitoring of tissue morphology and composition. Changes in synovial appearance, such as turbidity, vascularization, or structural alterations, can be captured in situ, while spectral signals provide complementary information on microbial presence and metabolic activity. The co-localization of sensing and emission ensures consistent spatial referencing between diagnosis and intervention.

From a therapeutic standpoint, embedded light sources enable localized treatment strategies within deep anatomical compartments. Direct intra-articular delivery allows confined irradiation with reduced input power while maintaining biologically effective doses, critical under implant-level energy and thermal constraints.

Importantly, the combination of spatial confinement and direct optical coupling enables precise control over irradiance, exposure time, and emission geometry. This control is essential to balance antimicrobial efficacy with tissue safety, particularly for high-energy modalities such as ultraviolet radiation, while ensuring stable operation in lower-energy regimes.

Taken together, optical accessibility is not merely a material property but a system-level design feature that enables co-localized sensing and therapy within a confined biological environment, forming the physical foundation of a truly theranostic implant system.

2.3. Enabling Light-Based Therapeutic Modalities

The integration of optoelectronic components within the SmartSpacer platform enables the implementation of multiple light-based therapeutic modalities, each addressing different aspects of infection control.

Visible light, particularly in the blue spectral range, can be applied to modulate bacterial metabolism and inhibit growth through photochemical mechanisms.[47,48] In contrast, ultraviolet radiation provides a direct bactericidal effect by inducing DNA damage, enabling rapid reduction of bacterial load.[49] Beyond these individual modalities, the system also allows combination approaches, in which light exposure enhances antibiotic susceptibility or disrupts biofilm integrity.

This latter aspect is of particular importance in the context of periprosthetic joint infection, where biofilm formation on implant surfaces represents a central mechanism of persistence and treatment failure. Bacteria embedded in biofilms exhibit significantly increased tolerance to antibiotics and host immune responses, making eradication difficult with conventional strategies alone.[50] Light-based interventions offer a complementary mechanism by directly targeting biofilm structure, increasing permeability, and sensitizing bacteria to antimicrobial agents.

 doi:10.20944/preprints202604.1875.v1

In addition, emerging evidence from preclinical and early clinical research indicates that light-based approaches can be effective against multidrug-resistant pathogens and biofilm-associated infections, further highlighting their relevance for implant-related complications.[51] These findings position optical therapy not merely as an adjunct, but as a potentially critical component in addressing some of the most challenging infection scenarios in modern medicine.

Crucially, these modalities address a key limitation of conventional treatment strategies: while antibiotic release from PMMA spacers is largely confined to an initial phase and declines significantly after approximately 2 days, the spacer remains implanted for substantially longer periods. Light-based interventions therefore provide a mechanism to extend active antimicrobial treatment beyond the passive diffusion window and to repeatedly target residual or biofilm-embedded bacteria throughout the implantation period.

The selection and implementation of these modalities are governed by a balance between antimicrobial efficacy and tissue safety, as well as by the technical constraints of the implant. Rather than relying on a single mechanism, the platform is inherently designed to support complementary and potentially synergistic treatment strategies, enabling adaptive and localized infection control directly at the implant–tissue interface.

2.4. Engineering Constraints and Design Considerations

The realization of light-based therapy within an implantable system introduces a set of stringent engineering constraints that fundamentally shape the feasible design space.

Energy availability is inherently limited, necessitating the use of highly efficient light sources and optimized operational strategies such as pulsed or duty-cycled emissions. At the same time, thermal management is critical to prevent local tissue damage and ensure device stability. Spatial constraints impose strict requirements on miniaturization and integration density, while maintaining robustness under mechanical load.

These constraints must be considered in the context of clinically relevant implantation durations, which can extend from several weeks to up to three months, thereby requiring long-term stability of both electronic components and therapeutic functionality.

In addition, regulatory considerations, particularly regarding electromagnetic exposure, device safety, and biocompatibility, must be addressed from the earliest stages of system design.

These factors collectively require a translation-oriented evaluation of therapeutic approaches, in which biological efficacy is considered alongside technical feasibility and system-level integration.

From an engineering perspective, the feasibility of light-based therapy within an implantable system is fundamentally governed by quantitative constraints on energy delivery and thermal stability. The current platform integrates multiple miniaturized light sources with a combined radiant output on the order of about 30 mW (with current LEDs). Optical coupling efficiencies in the range of approximately 10–15% result in several milliwatts of effective power available for localized interaction within the joint environment.

Thermal characterization under representative operating conditions indicates temperature increases below 0.2 °C, even during peak activity phases. This minimal thermal footprint reflects both the efficiency of modern solid-state light sources and the buffering capacity of the surrounding tissue, and remains well within physiologically acceptable limits for repeated or continuous operation.

In parallel, experimentally reported antimicrobial thresholds, particularly in the ultraviolet regime, typically fall within the range of approximately 0.3–3,0 mJ cm^{-2} for measurable bactericidal effects. While instantaneous delivery of such doses remains constrained by implant-level power budgets, these values are compatible with pulsed or duty-cycled emission strategies over clinically relevant time scales.[52]

Taken together, these considerations define a quantitatively bounded yet practically accessible operating space, in which biologically relevant optical effects can be achieved under the strict energy and safety constraints of an implantable system.

 doi:10.20944/preprints202604.1875.v1

2.5. From Concept to Translational Framework

This work does not review light therapy per se, but defines a translation-oriented framework for its implementation in implantable systems.

The SmartSpacer platform thus provides a concrete technological foundation for implementing theranostic concepts in orthopedic infection management. By combining continuous sensing with controllable light-based therapy, it enables a fundamentally new approach to treatment.

Rather than relying on passive drug release and indirect diagnostics, the system allows active, localized, and adaptive intervention directly within the joint space. This transformation from static to dynamic therapy forms the basis for the subsequent analysis presented in this work.

In the following sections, light-based antimicrobial strategies are systematically evaluated with respect to their suitability for integration into such a platform, with particular emphasis on wavelength-dependent effects, energy requirements, and translational feasibility.

Rather than providing a comprehensive overview of light-based antimicrobial approaches, this work focuses on the definition of a translation-oriented framework for their implementation within implantable systems. Emphasis is placed on identifying feasible operating regimes under realistic constraints, linking biological mechanisms to engineering design principles.

In the following sections, light-based antimicrobial strategies are systematically evaluated with respect to their suitability for integration into such a platform, with particular emphasis on wavelength-dependent effects, energy requirements, and translational feasibility.

This work defines the first translation-oriented design framework for implementing light-based antimicrobial therapy within implantable systems.

3. From Descriptive Review to Translational Framework

Conventional reviews on light-based antimicrobial therapies primarily focus on biological efficacy, experimental protocols, and mechanistic insights. While essential for understanding light–microbe interactions, they provide limited guidance for the development of implantable therapeutic technologies.

In the context of PJI, the key question is not whether a given approach is effective under controlled conditions, but whether it remains implementable within a constrained implant environment, where energy, space, and safety margins are inherently limited.

To address this gap, this work adopts a translation-oriented framework that shifts the focus from descriptive analysis to system-level applicability. Representative studies are selectively analyzed to extract parameters directly relevant for implementation in a theranostic implant system such as the SmartSpacer.

3.1. Translational Selection and Parameter Mapping

Study selection is guided by a dual criterion combining biological validity and technical feasibility. Included studies must demonstrate reproducible antimicrobial effects, such as growth inhibition, biofilm disruption, or bactericidal activity, particularly against clinically relevant PJI pathogens, including Staphylococcus aureus, Staphylococcus epidermidis, and antibiotic-resistant strains.

Equally, the investigated approaches must be compatible with implant constraints, including energy efficiency, thermal behavior, spatial integration, and applicability within confined anatomical environments. Strategies requiring excessive energy input, significant heat generation, or impractical delivery geometries are excluded.

To enable systematic comparison across heterogeneous studies, key parameters are extracted and mapped into a common design space. These include wavelength, energy density, irradiance, exposure time, and treatment regime, as well as the biological target (planktonic bacteria vs. biofilms). Rather than treating these variables independently, they are interpreted in relation to each other, allowing experimental outcomes to be translated into implementable operating regimes.

 doi:10.20944/preprints202604.1875.v1

3.2. Integration of Engineering Constraints

A defining feature of this framework is the explicit integration of engineering constraints. Implantable systems operate under tightly bounded conditions that fundamentally shape the feasible solution space.

Energy must be distributed across sensing, processing, and therapy, while thermal effects must remain within safe limits to prevent tissue damage. Device size and integration density are constrained by anatomical and mechanical requirements, and material properties influence both optical transmission and long-term stability.

These constraints must be considered over clinically relevant implantation periods, typically several weeks (2–6 weeks) up to approximately 3 months, requiring sustained functionality under limited energy budgets. In addition, regulatory requirements impose strict limits on electromagnetic exposure and device safety, further restricting the permissible operating range.[53–56]

3.3. From Experimental Evidence to Design Rules

The objective of this methodology is not merely comparative, but generative: to derive actionable design principles for theranostic implant systems.

By abstracting experimental results into parameter spaces defined by wavelength, energy, and biological effect, feasible operating regions can be identified. This enables differentiation between modalities suitable for continuous operation, pulsed intervention, or combined strategies.

Crucially, this transformation links biological mechanisms directly to engineering implementation, enabling a systematic, design-driven approach to therapy development.

4. Spectral Design Space for Light-Based Antimicrobial Therapy

The therapeutic use of electromagnetic radiation for antimicrobial applications is governed by a multidimensional design space defined by wavelength, energy density, and exposure dynamics. In implantable systems, this space is further constrained by the intersection of achievable dose, thermal limits, and available power. Accordingly, the central question is not which wavelengths are effective in principle, but which wavelength–dose combinations remain implementable within an implant-level energy budget.

Within the SmartSpacer platform, optical power at the tissue interface is on the order of ~5 mW, restricting operation to low fluence regimes and necessitating efficient temporal modulation strategies. Experimental observations indicate that antimicrobial effects can, depending on the wavelength, be induced at energy densities in the low mJ cm^{-2} range, thereby defining a practically accessible intervention window under implant constraints. This establishes a translation-oriented design space in which antimicrobial effects must be considered jointly as a function of wavelength and energy density, bounded by system-level limitations. Within this regime, both continuous and pulsed strategies become feasible, enabling a transition from static treatment concepts toward dynamic, implant-driven infection control.

To systematically structure this multidimensional design space, Table 3 provides a comparative overview of representative wavelength regimes, associated energy ranges, and their experimentally observed biological effects. Rather than offering an exhaustive compilation, the selection is guided by translational relevance, focusing on studies and parameter ranges that are compatible with implant-level constraints. The table integrates data across ultraviolet, visible, and near-infrared spectral domains and relates them to their dominant antimicrobial or host-modulatory mechanisms, typical dose ranges, and experimental contexts.

Table 3. Wavelength-dependent biological effects of electromagnetic radiation; Summary of selected studies across UV, visible, and near-infrared spectral ranges, highlighting wavelength-specific antimicrobial effects and host tissue responses under conditions compatible with implant-based application. Studies were specifically

 doi:10.20944/preprints202604.1875.v1

chosen based on their relevance to energy, power density, and exposure constraints feasible within the SmartSpacer platform.

IR (>780 nm)					
IR 1064 nm	~10 mW/cm²	Endothelial cells	higher NO release, higher Akt & eNOS phosphorylation, mitochondrial involvement	In-vitro	[57]
IR 980 nm	~5–50 J/cm²	Muscle tissue / inflammation	Anti-inflammatory effects, reduced oxidative stress, improved tissue regeneration	In-vivo	[29]
IR 830 nm	1–20 J/cm²	Wound healing (fibroblasts, keratinocytes)	Enhanced proliferation, collagen synthesis, accelerated wound healing	In-vivo	[67]
IR 808 nm	~1–10 J/cm²,	Human fibroblasts / mitochondrial activity	Increased ATP production, enhanced proliferation, activation of cytochrome c oxidase	In-vitro	[69]
VIS (380-780 nm)					
VIS 470 nm 660 nm	5 mW, 6 hours 284.90 J/cm², 603.44 J/cm²	Inhibition of Staphylococcus aureus and Pseudomonas aeruginosa growth	Blue light, but not red light, can temporarily inhibit the growth of gram-negative and gram-positive bacteria.	In-vitro	[47]
VIS 420 nm 635 nm	Twice daily 72 J/cm² 43.8, 87.6, and 175.5 J/cm²	Candida albicans biofilm matrix development	Affects biofilm development and physiology of polysaccharide production	In-vitro	[70]
VIS blue only (400-500 nm)					
VIS 470 nm	16.29, 27.16 and 54.32 J/cm²	Staphylococcus aureus growth delay	Inhibitory effect but not absolute antibacterial	In-vitro	[48]
VIS 450-470 nm	60–240 J/cm²	Candida albicans elimination	460 nm eradicates planktonic and biofilm Candida albicans	In-vitro, In-vivo Animal	[71]
VIS 450 nm	With riboflavin: 15, 30, 56, and 84 J/cm²	Effects on MRSA and human keratinocytes	• High doses blue light could treat infections without harming skin cells, • PDT with riboflavin is promising	In-vitro	[72]
VIS 412 nm, 450 nm	With riboflavin 5.4 J/cm² and 28.5 J/cm²	MRSA eradication	Riboflavin enhances the antibacterial effect of blue light	In-vitro	[73]
VIS 405 nm, 450 nm	300 J/cm² 400 J/cm² (1000 J/cm²)	Effect on ESKAPE pathogens and human cells	Significant reduction in viable bacteria	In-vitro	[74]

 doi:10.20944/preprints202604.1875.v1

VIS 405 nm ± 3 nm	Continuous visible light over 72 hours 0.34–0.44 mW/cm²	Antimicrobial activity against • C. difficile • MRSA • VRE • MDR Acinetobacter baumannii	• The high irradiant light significantly reduced both vegetative bacteria and spores • Over a 72-hour exposure period.	In-vitro	[75]
VIS 405 nm	144 J/cm²	Antimicrobial action in stored plasma	• Decontaminates pre-bagged plasma without photosensitizing agents • 99.9% reduction of low-density bacterial populations • 405 nm light application provides new proof of concept for bacterial reduction in biological fluids	In-vitro	[76]
VIS 405 nm	• Overview of the mechanisms of 405 nm for environmental decontamination • Different energy densities	Pathogen inactivation Environmental disinfection	• Significant antimicrobial properties for environmental disinfection • Even in crowded working areas	In-vitro	[77]
VIS 400-420 nm	350–400 mW/cm²	Staphylococcus aureus inactivation	Maximum inactivation at 405±5 nm	In-vitro	[78]
VIS 380-480 nm	Up to >1500 J/cm²	Review of the last thirty years Microbial species susceptibility	Higher doses needed for longer wavelengths	In-vitro	[79]
UVA (380–315 nm)					
UV-A, B, C, blue light pulsed blue light (PBL)	Different UV doses and PBL	Overview of various methods for photo eradication of microorganisms (SARS-CoV-2)	• UV-C is highly effective, followed by UV-B, UV-A, • UV-C minimal depth penetration in humans • The damaging effect of UV was more significant with UV-B than with UV-C • High potency of PBL at each of the violet-blue wavelengths makes it significantly more germicidal at lower irradiances and fluences than CW light	In-vitro, In-vivo Clinical & animal	[80]
UVA: 343-375 nm UVB: 280-313 nm	Various applications and energy densities	Comparison and overview of possible wavelength ranges and energy densities for in vivo disinfection	• UV irradiation shows a significant potential of being an effective therapy method for infectious diseases. • UV irradiation in different wavelength bands can inactivate	In-vivo Clinical & animal	[52]

 doi:10.20944/preprints202604.1875.v1

UVC: 222-254 nm			microbes based on different mechanisms		
UV-A, B 300-380 nm	Depending on Fitzpatrick skin types Up to 5000 mJ/cm²	Psoriasis and Vitiligo treatment	• Effective for treating dermatoses	In-vivo Clinical	[81]
UVA peak at 400 nm	3 mW/cm², 30 + 30 min	Vulvovaginal candidiasis	Patients with vulvovaginal candidiasis present a reduction of inflammation and disappearance of symptoms of pruritus and burning after a treatment.	In-vivo Clinical	[82]
UVA peak at 343 nm	2.0 mW/cm², 30 min, or 3.0–3.5 mW/cm², 20 min daily for 2 d	• Multiple bacteria, yeast, and viruses (in vitro) • Safety study (in vivo)	• UVA exposure demonstrates effective inactivation of various bacteria, yeast, and viruses • Single and repeated UVA irradiation is safe for mice based on the endoscopic examination and full-thickness pathologic assessment results	In-vivo Animal	[83]
UVA peak at 343 nm	2 mW/cm², 20 min daily for 5 d	SARS-CoV-2 infection	• Four out of five subjects clinically improved on day 30 after the treatment. • Endotracheal UVA phototherapy under specific conditions was safe for humans with a significant reduction in respiratory SARS-CoV-2 viral load	In-vivo Clinical	[84]
UVB (315–280 nm)					
UVB 300 nm	300 nm	Epidermal absorbers	Major absorbers include aromatic amino acids, nucleic acids, urocanic acid, and melanin.	In-vivo Clinical	[85]
UVB peak at 313 nm	250–1500 J/cm²	AMP expression	• Expression of AMPs were detected on all subjects • hBD-2 expression was detected only on one subject	In-vivo Clinical	[86]
UVB 280-315 nm	2.3 mW/cm²	AMP expression	hCAP18 was found to be expressed significantly in the human skin	In-vivo Clinical	[87]
UVB peak at 313 nm	40 mJ/cm² daily for 1 or 3 d	AMP expression	Expression of mBD-3, cathelin-related antimicrobial peptide, and LL-37 were observed	In-vivo Animal	[88]
UVB peak at 311 nm	Up to 1.6 J/cm²	Atopic eczema	UVB irradiation can modulate the expression of hBD-1 and hBD-2 for atopic eczema	In-vivo Clinical	[89]
UVB peak at 311 nm	0.13–8.88 J/cm²	Atopic dermatitis and psoriasis	Enhanced expression of LL-37 and decreased expression of hBD-2 after UVB treatment,	In-vivo Clinical	[90]

 doi:10.20944/preprints202604.1875.v1

			significant improvement of psoriasis and atopic dermatitis		
UVB peak at 306 nm	1.68 J/cm²	Atopic dermatitis with S. aureus and S. epidermidis	• The UVB irradiation shows an excellent antimicrobial effect against S. aureus, • But no effect on S. epidermidis	In-vivo Clinical	[91]
UVB 4.3 J accumulated	4.3 J accumulated	Atopic dermatitis with S. aureus	UVB irradiation demonstrates a significant suppression of superantigen production from S. aureus in patients with atopic dermatitis	In-vivo Clinical	[92]
UVC (280–100 nm)					
UVC 254 nm	30 minutes after the inoculation 3.24 J/cm² for abrasions and 2.59 J/cm² for burns	Acinetobacter baumannii wound infections	• DNA lesions were observed immediately after a UVC exposure • The lesions were extensively repaired within 72 hours.	In-vivo Animal	[49]
UVC 254 nm 265 nm 280 nm	4, 8,11,14 mJ/cm² 1,3, 2,5 3,8, 5,1 mJ/cm² 15,30,45,60 mJ/cm²	SARS-CoV-2 inactivation via different sources	• 265-nm deep UV light-emitting diode (DUV-LED) lamp efficiently inactivated SARS-CoV-2 • At a similar level as a 254-nm • And at a higher level than a 280-nm	In-vitro	[93]
UVC 207 nm	157 mJ/cm²	• infection reduction • Safety study	Potential use for antimicrobial properties without hazards to skin	In-vivo Animal	[94]
UVC peak at 254 nm	2.7 mW/cm², 18 min on day 0, or 40 min on day 1	• C. albicans burn infection in mice • Safety study	• Exposure on day 0 gives a 99.2% reduction of fungal burden, exposure on day 1 gives a 95.8% reduction of fungal burden • CPD were observed by immunofluorescence in normal mouse skin immediately after UV irradiation, and the damage was extensively repaired within 24 h	In-vivo Animal	[95]
UVC peak at 254 nm	2.7 mW/cm², 16 min	• P. aeruginosa and S. aureus cutaneous wound infections in mice • Safety study	• A 10-fold reduction of the P. aeruginosa and S. aureus burden on mice skin • CPD-positive nuclei were observed in the immunofluorescence micrograph of mouse skin, and the damage was extensively repaired within 48 h	In-vivo Animal	[96]

 doi:10.20944/preprints202604.1875.v1

UVC peak at 254 nm	180 s; 7 treatments over 14 d + 4 treatments over 1 month	MRSA-infected chronic ulcer on human	• UVC irradiation reduced wound bacterial burden and facilitated wound healing for all three patients • Two patients had complete wound closure following 1 week of UVC irradiation	In-vivo Clinical	[97]
UVC peak at 222 nm & peak at 254 nm	40 mJ/cm² and 300 mJ/cm²	• MRSA infected superficial skin wound of mice • Safety study	• Both 222 and 254 nm irradiation show a statistically significant reduction of bacteria counts on days 2 and 7 • 222 nm light showed the same bactericidal properties of 254 nm light but without the associated skin damage (CPD formation)	In-vivo Animal	[98]
UVC peak at 233 nm	44 μW/cm² 15–40 mJ/cm²	• A skin tolerant far-UVC (< 240 nm) irradiation system • Inactivation of MRSA	• Porcine skin showed only 3.7% CPD and 2.3% 6-4PP DNA damage • Corresponding irradiation at 254 nm caused 11–14 times higher damage • skin damage is so small that it can be expected to be compensated by natural repair mechanisms	In-vitro	[99]
UVC peak at 233 nm	40 mJ/cm²	• Eradication of MRSA, MSSA, SE and risk assessment on skin	• 5 log10 levels reduction without no soil load • 1.5–3.3 with soil load • DNA damage was far below the damage evoked by 0.1 UVB minimal erythema dose • far lower than 20 min outdoor visible light	In-vitro	[100]
UVC peak at 233 nm	60 mJ/cm²	• Safe inactivation of multi-resistant nosocomial pathogens	• reduced by ≈ 5 log10 for 60 mJ/cm² • DNA damage occurred only superficially and decreased after 24 h • < 10% of keratinocytes were affected	In-vitro	[101]
UVC peak at 222 nm	75, 150, and 450 mJ/cm²	• MRSA-infected skin wound of mice • Safety study	• 222 nm irradiation shows a significant bactericidal effect, which was equal to or more effective than 254 nm irradiation • CPD-expressing cells were found in both epidermis and dermis with 254 nm	In-vivo Animal	[102]
UVC peak at 222 nm	50–500 mJ/cm²	• Bactericidal effect on healthy human skin • Safety study	• The number of bacterial colonies in the skin swab culture was reduced significantly • The CPD amount produced in the irradiated region	In-vivo Clinical	[103]

 doi:10.20944/preprints202604.1875.v1

				was slightly but significantly higher than that of the non-irradiated region		
UVC peak at 222 nm & peak at 254 nm	157 mJ/cm², delivered in 7 h	• MRSA (in vitro) • Safety study (in vivo)		• Both 254 and 222 nm irradiation can kill MRSA efficiently • ,Unlike 254 nm, 222 nm UVC irradiation is safe for mouse skin, and no detectable formation of mutagenic CPDs was observed	In-vivo Animal	[104]

In doing so, it establishes a practical mapping between fundamental photobiological effects and their feasibility within the limited power and thermal budget of an implantable system such as the SmartSpacer. This structured overview serves as the basis for identifying implementable wavelength–dose combinations and for defining operational strategies that balance antimicrobial efficacy with in vivo safety.

4.1. Wavelength-Dependent Antimicrobial Mechanisms

The antimicrobial effects of electromagnetic radiation are strongly wavelength-dependent, reflecting distinct interaction mechanisms with biological systems. For implantable applications, wavelength primarily determines interaction depth and mechanism, while energy density governs the magnitude and nature of the induced response.(Figures 4 and 5)

In the UVC regime (~200–280 nm), absorption by nucleic acids results in direct DNA damage and rapid bacterial inactivation at low energy densities.[49] This enables highly efficient bactericidal action, but within a narrow therapeutic window due to comparable effects in host tissue. As a result, implant-based UVC application requires strictly controlled, pulsed operation.

In contrast, visible blue light (≈405–470 nm) induces antimicrobial effects via photochemical excitation of endogenous chromophores, such as porphyrins.[48] This process leads to the generation of reactive oxygen species (ROS), which disrupt bacterial metabolism, membrane integrity, and intracellular pathways. These mechanisms result in dose-dependent growth inhibition rather than immediate eradication and are compatible with continuous or duty-cycled operation under low thermal load.

At longer wavelengths (green to near-infrared), direct antimicrobial effects decrease substantially, while interactions increasingly shift toward modulation of host cell physiology, including regenerative and anti-inflammatory processes.[57] From a translational and engineering perspective, these wavelength-dependent effects impose both constraints and opportunities. Certain interactions, such as nonspecific DNA damage in host tissue, must be strictly minimized, while others, such as ROS-mediated bacterial sensitization or host-regenerative responses, can be selectively exploited. Consequently, a careful balance between therapeutic efficacy and biological safety must be achieved for in vivo application.(Table 2)

Within this framework, different spectral regimes define complementary operational modes that can be strategically combined. High-energy, pulsed UVC exposure enables rapid bactericidal interventions, whereas lower-energy visible light supports continuous antimicrobial suppression via ROS generation. Simultaneously, longer wavelengths in the red to near-infrared range can promote tissue regeneration and modulate inflammation.(Figure 6)

Taken together, the relevant wavelength ranges, frequency bands, and associated energy regimes delineate a multi-modal design space for implant-based phototherapy. Within the constrained implant-operating window, these modalities can be integrated into a unified system-level approach that combines pulsed bactericidal action with continuous suppression and host-directed modulation, thereby enabling controlled and localized infection management.

 doi:10.20944/preprints202604.1875.v1

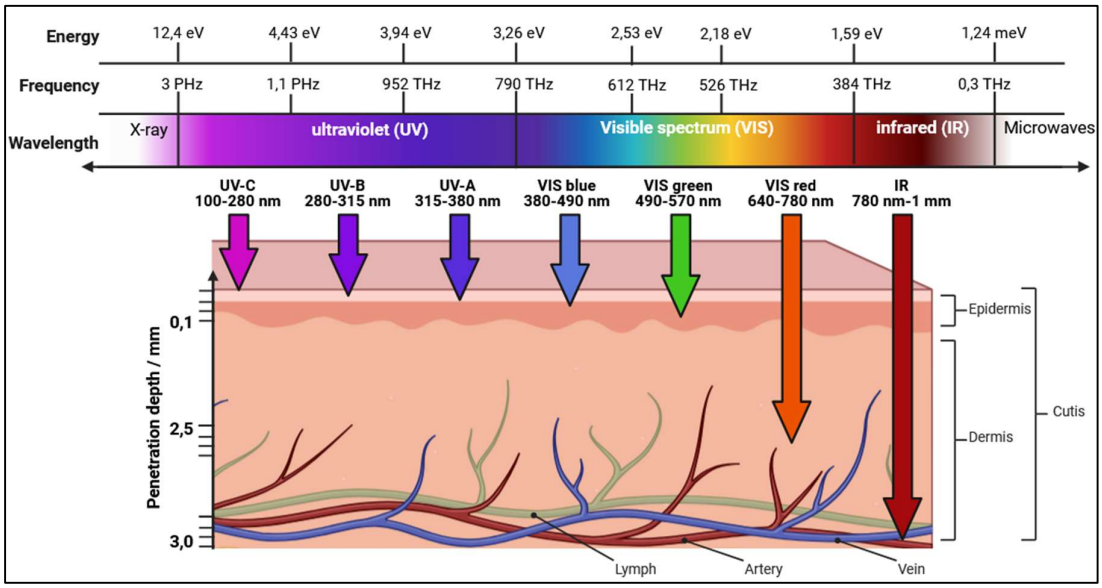

Figure 4. Representation of the different effects on biological tissues at the corresponding energy densities, plotted on an irradiance versus exposure time diagram, with the major energy barriers indicate.

Table 2. List of different effects of the relevant wavelengths on human cells and bacteria.[29,58–68].

UV-C	UV-B	UV-A	VIS blue	VIS green	VIS red	IR
Effect on human cells						
Causes DNA changes	Acute damage: main cause of sunburn.	Long-term damage: Causes skin ageing, can increase the risk of skin cancer	Increase in nitric oxide	Improvement of differentiation and matrix mineralisation of osteogenic cells	Enhancement of cell proliferation (by suppressing cell apoptosis)	Induction of regenerative and anti-inflammatory effects
Changes the barrier function of cells	Long-term effects: DNA damage and increase the risk of skin cancer	Immediate effects: May cause sunburn, although less energetic	Molecular and cellular changes in fibroblasts	Support of healing processes through mitochondrial stimulation and increase in ATP	Modulation of cell growth	Increase in collagen production in dermal fibroblasts
Can lead to cell necrosis	Vitamin D production in the skin, for bone health & immune system	Vitamin D synthesis: Contributes to the production of vitamin D	Premature skin ageing	Hardly harmful Effect on skin and eyes: Compared to blue light	Enhancement of succinic dehydrogenase activity	Change in the collagen balance of the extracellular matrix of the skin
Effect on bacteria						
Direct DNA destruction of the bacteria leads to immediate cell death	Direct DNA damage to the bacteria prevents correct replication and	Indirekt DNA-Schäden indem es reaktive Sauerstoffspezies (ROS) erzeugt	Strong bactericidal effect	Moderate bactericidal effect	Reduced bactericidal effect	Low direct bactericidal effect

 doi:10.20944/preprints202604.1875.v1

	leads to mutations					
Cell wall and membrane damage leads to loss of structural integrity and cell death	Protein modification leads to impairment of cell functions	ROS-Angriff auf Zellmembran führt zu erhöhter Permeabilität und Zelltod führen	Formation of reactive oxygen species (ROS)	Destabilisation of the cell membrane	Influencing cell proliferation	Often in combination with photosensitisers
Inactivation of enzymes leads to a halt in metabolic processes	Stress response leads to the production of protective proteins and damage is repaired	Stress response leads to the production of protective proteins and damage is being repaired	Damage to the cell membrane and DNA	Inhibition of cell division	Damage to the cell membrane due to thermal effects	Influenced by thermal effects, increase in permeability

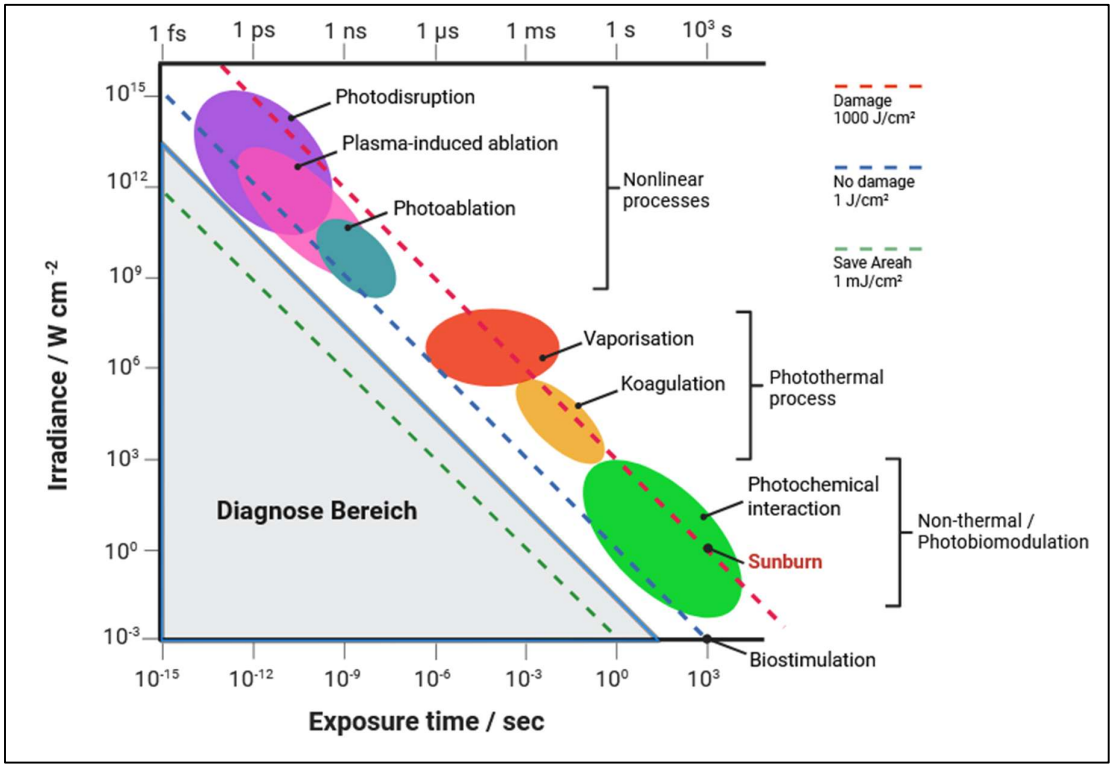

Figure 5. Illustration of the different wavelength ranges of interest with details of their penetration depth into the skin, frequency bands and energy levels.

 doi:10.20944/preprints202604.1875.v1

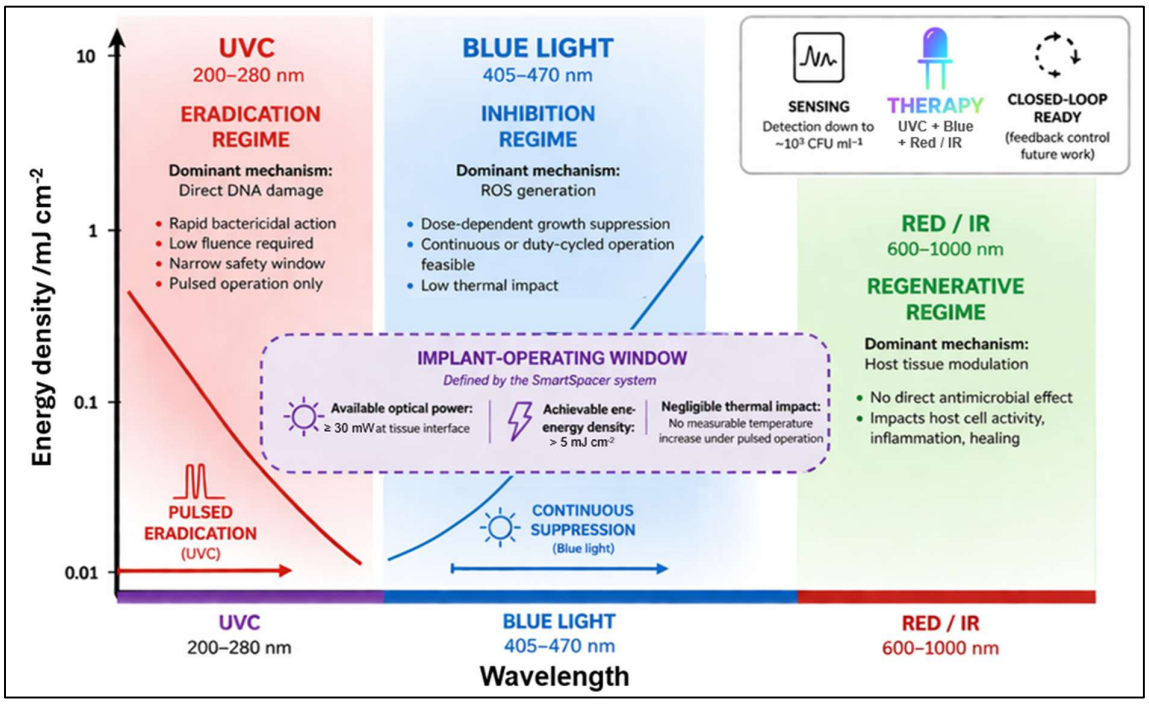

Figure 6. Translation-oriented design space for implantable light-based antimicrobial therapy. Antimicrobial effects are mapped as a function of wavelength and energy density, highlighting UVC-driven bactericidal regimes and blue-light-mediated ROS inhibition. The shaded region indicates the implant-operating window defined by limited optical power (≥30 mW) and low achievable energy densities (>5 mJ cm^{-2}), within which continuous and pulsed treatment strategies can be combined.

4.2. Visible Light: Inhibition-Dominated Regime

Within the visible spectrum, blue light represents the most relevant regime for implantable antimicrobial applications. Exposure in the range of 405–470 nm consistently induces growth suppression across clinically relevant pathogens, primarily through oxidative stress mechanisms.[47]

However, this effect is inherently dose-dependent and typically does not result in complete bacterial eradication. Instead, it induces a controlled reduction in proliferation and metabolic activity.

From an engineering perspective, this regime is highly compatible with implant constraints. Light sources are energy-efficient, thermal effects are negligible, and operation can be sustained over extended periods.

Implication for implant design:

Blue light is optimally suited for continuous or duty-cycled baseline therapy, stabilizing the infection environment rather than achieving immediate eradication.

4.3. Low-Fluence Regimes and Continuous Operation

At low energy densities, blue light induces transient antimicrobial effects that are insufficient for sustained bacterial suppression. However, the minimal energy requirements and absence of thermal load make this regime uniquely suitable for continuous operation.[48]

This introduces a critical trade-off: while higher fluence increases efficacy, it is often incompatible with implant-level power constraints. Conversely, low-fluence regimes enable long-duration application with minimal risk.

Within an implant-based system, this favors a strategy based on cumulative dosing rather than peak intensity.

 doi:10.20944/preprints202604.1875.v1

Implication for implant design:

Low-fluence visible light should be implemented as a continuous background therapy, leveraging cumulative effects while remaining within strict energy and thermal limits.

4.4. Ultraviolet Radiation: Eradication-Dominated Regime

Ultraviolet radiation, particularly in the UVC range (~200–280 nm), enables rapid bacterial inactivation through direct DNA damage. Experimental evidence indicates that measurable antimicrobial effects can occur at energy densities around 3J cm^{-2} DNA lesions were repaired within 72 hours.[49]

This high efficacy contrasts with a narrow therapeutic window, as similar mechanisms affect host tissue. As a result, exposure must be tightly controlled in both time and space.

Within implantable systems, continuous operation is not feasible due to safety and energy constraints. Instead, therapeutic application must rely on temporally structured delivery.

Implication for implant design:

UVC should be implemented as a pulsed, high-impact intervention for targeted bacterial reduction, compatible with implant-level power (>5 mW) and controlled via short exposure cycles.

4.5. Functional Complementarity Across Spectral Regimes

A key insight is that different wavelength regimes fulfill complementary rather than competing roles. Visible light enables sustained modulation of bacterial dynamics, while ultraviolet radiation provides rapid reduction of bacterial load.

This functional separation aligns naturally with implant constraints, where neither continuous high-intensity irradiation nor single-modality approaches are feasible.

Implication for implant design:

Effective therapy requires a dual-regime strategy combining continuous visible-light suppression with intermittent UVC-based eradication.

4.6. Implications for Implant-Based Therapy Design

Taken together, these findings define a translation-oriented design principle: implant-based infection control must rely on the coordinated use of complementary light modalities operating within a constrained energy envelope.

Within the SmartSpacer platform, optical power levels of >5 mW at the tissue interface, combined with pulsed operation and negligible thermal load, enable both continuous low-intensity and intermittent high-impact treatment strategies.

This establishes a multi-layered therapeutic architecture in which visible light provides baseline stabilization, ultraviolet radiation enables targeted eradication, and sensing data guides temporal application.

Rather than maximizing instantaneous efficacy, the system operates within a bounded but effective regime defined by power, dose, and temporal control.

Implication for implant design:

Therapeutic performance emerges not from a single modality, but from the integration of wavelength-specific functions within a unified, energy-constrained system.

5. Synergistic Effects and Combination Therapy

Monomodal antimicrobial strategies, whether antibiotic-based or light-based, are inherently limited in achieving robust infection control in complex environments such as periprosthetic joint infections. Antibiotics suffer from restricted biofilm penetration and temporally limited release, with diffusion from PMMA spacers largely declining after ~2 days, resulting in prolonged sub-therapeutic exposure. Similarly, isolated light-based approaches are constrained by wavelength-specific limitations.

 doi:10.20944/preprints202604.1875.v1

Recent evidence demonstrates that combining light-based modalities with conventional antimicrobials enables synergistic effects beyond simple additivity. Light-induced oxidative stress disrupts bacterial structures and metabolic pathways, increasing susceptibility to antibiotics, while concurrent biofilm weakening facilitates deeper drug penetration. Sub-lethal irradiation can further enhance bacterial metabolic activity, improving responsiveness to antibiotics targeting active processes.

These interactions result in over-additive therapeutic effects, enabling reduced antibiotic dosage, lower systemic exposure, and improved efficacy against resistant and biofilm-associated pathogens.

Beyond direct antimicrobial action, longer wavelengths in the red and near-infrared range introduce complementary host-mediated effects. Photobiomodulation enhances cellular metabolism, mitochondrial function, and tissue regeneration, supporting wound healing, immune response, and microcirculation.

From a systems perspective, this enables a shift from purely antimicrobial intervention to a combined anti-infective and regenerative strategy. Within the SmartSpacer framework, continuous low-intensity visible light can suppress bacterial growth, while pulsed ultraviolet exposure provides targeted bactericidal action. Concurrent antibiotic therapy is enhanced through light-induced sensitization, and red to near-infrared irradiation supports tissue recovery.

Together, this integrated, multi-modal approach enables a transition from isolated treatments to coordinated therapy, combining antimicrobial and regenerative mechanisms to achieve superior outcomes within the constraints of an implantable system.

6. Toward In Vivo Implementation

Central to in vivo implementation is the definition of therapeutic operating windows that balance antimicrobial efficacy with tissue safety and system constraints. Within the SmartSpacer platform, optical power levels of up to >5 mW can be delivered at the implant–tissue interface. Pulsed operation prevents cumulative thermal buildup, resulting in negligible temperature increases under representative conditions. Experimental observations indicate that antimicrobial effects can be achieved at energy densities as low as ~0.45 mJ cm^{-2}, supporting feasibility within implant-level energy budgets.

A key enabler is continuous, localized biomarker acquisition. The system integrates high-resolution temperature sensing (±0.1 °C), optical monitoring of tissue morphology, and spectral detection of bacterial load down to ~10^3 CFU ml^{-1}, enabling direct intra-articular assessment of infection. Crucially, diagnostic value arises from longitudinal analysis: time-resolved trends allow differentiation between physiological variability and pathological change. Stable baselines indicate absence of infection, whereas subtle deviations, such as gradual temperature increases or spectral shifts, enable early detection prior to clinical manifestation.

This data-driven framework enables adaptive therapy. Visible light, particularly in the blue range, supports continuous or repeated application due to its favorable safety profile and low thermal impact. In contrast, ultraviolet radiation requires precise, pulsed delivery within a narrow therapeutic window. Real-time biomarker feedback allows dynamic adjustment of these modalities, enabling a transition from static protocols to adaptive intervention strategies.

From an engineering perspective, system performance is governed by strict constraints on energy, thermal behavior, and reliability. Efficient light sources, duty-cycled operation, and optimized data transmission ensure functionality within limited power budgets, while thermal increases remain minimal (<0.2 °C). These characteristics support stable operation over clinically relevant implantation periods of weeks to months.

Regulatory requirements impose additional constraints on safety, electromagnetic exposure, and biocompatibility, necessitating comprehensive risk assessment. However, continuous local monitoring also enables enhanced safety through feedback-controlled operation.

Together, these elements establish a technological foundation for feedback-driven infection management. While fully autonomous control remains future work, the integration of continuous

 doi:10.20944/preprints202604.1875.v1

sensing with controllable light-based therapy represents a critical step toward adaptive, patient-specific treatment.

7. Future Perspective: Toward Theranostic Infection Control

The integration of sensing and therapy within a single implant platform enables a fundamental shift toward closed-loop infection management. In such systems, continuous monitoring of local conditions provides real-time information that can be used to dynamically adjust therapeutic interventions, creating a feedback-driven treatment paradigm.

This approach transforms implants from passive structural elements into active therapeutic systems capable of interacting with their biological environment. In the context of periprosthetic joint infection, this enables a transition from static treatment protocols toward adaptive strategies that respond to the evolving infection state.

While the SmartSpacer represents a specific implementation within orthopedic surgery, the underlying concept is broadly applicable to other medical domains. Implantable devices for infection control, wound management, or localized cancer therapy may benefit from similar integration of sensing and actuation.

Future work will focus on preclinical validation, optimization of treatment protocols, and the development of scalable system architectures. In particular, the integration of data-driven decision-making and advanced control strategies may further enhance the performance of theranostic implants.

This perspective positions theranostic systems as a key component of next-generation medical devices, enabling personalized, localized, and adaptive therapy.

Acknowledgements: The authors gratefully acknowledge financial support from the German Federal Ministry of Education and Research (BMBF) under the project “Smart wireless implant for infection monitoring – Development of a miniaturized sensor system” (FKZ: 01EK2107A). The authors thank all collaborators and supporting staff involved in the development of the SmartSpacer platform, in particular for contributions to system integration, experimental validation, and clinical input. The authors further acknowledge Essentim GmbH for contributions to PCB design and electronic system development, as well as Heraeus Medical for support related to bone cement materials. Special thanks are extended to the clinical and technical teams at the Technical University of Munich for their continuous support and valuable discussions.

Funding: German Federal Ministry of Education and Research (BMBF), Smart wireless implant for infection monitoring - Development of a miniaturized sensor system (01EK2107A).

Data Availability Statement: The data that support the findings of this study are available from the corresponding author upon reasonable request. Due to the ongoing development of the SmartSpacer platform and associated intellectual property considerations, certain data are not publicly available. Additional information about the project and platform development can be found at https://bonesens.com/.

References

1 A.J. Tande and R. Patel, “Prosthetic joint infection,” *Clinical microbiology reviews*, no. 27 (2014): 302-345. https://doi.org/10.1128/CMR.00111-13

2 S.M. Kurtz, I. Exponent, Philadelphia, Pennsylvania, P. Drexel University, Pennsylvania et al., “Economic Burden of Periprosthetic Joint Infection in the United States,” *The Journal of Arthroplasty*, no. 27 (2012): 61-65.e61. https://doi.org/10.1016/j.arth.2012.02.022

3 W. Zimmerli, A. Trampuz and P.E. Ochsner, “Prosthetic-Joint Infections,” *New England Journal of Medicine*, no. 351 (2004): 1645-1654. https://doi.org/doi:10.1056/NEJMra040181

4 S. Kurtz, K. Ong, E. Lau et al., “Projections of Primary and Revision Hip and Knee Arthroplasty in the United States from 2005 to 2030,” *The Journal of Bone & Joint Surgery*, no. 89 (2007): 780-785. https://doi.org/10.2106/JBJS.F.00222

 doi:10.20944/preprints202604.1875.v1

5 M. Sloan, A. Premkumar and N.P. Sheth, "Projected Volume of Primary Total Joint Arthroplasty in the U.S., 2014 to 2030," *The Journal of Bone and Joint Surgery*, no. 100 (2018): 1455-1460. https://doi.org/10.2106/jbjs.17.01617

6 M.J. Prince, F. Wu, Y. Guo et al., "The burden of disease in older people and implications for health policy and practice," *The Lancet*, no. 385 (2015): 549-562. https://doi.org/10.1016/S0140-6736(14)61347-7

7 S.E. Vollset, E. Goren, C.-W. Yuan et al., "Fertility, mortality, migration, and population scenarios for 195 countries and territories from 2017 to 2100: a forecasting analysis for the Global Burden of Disease Study," *The Lancet*, no. 396 (2020): 1285-1306. https://doi.org/10.1016/S0140-6736(20)30677-2

8 S. Corvec, M.E. Portillo, B.M. Pasticci et al., "Epidemiology and new developments in the diagnosis of prosthetic joint infection," *The International journal of artificial organs*, no. 35 (2012): 923-934. https://doi.org/10.5301/ijao.5000168

9 K.L. Ong, S.M. Kurtz, E. Lau et al., "Prosthetic joint infection risk after total hip arthroplasty in the Medicare population," *The Journal of arthroplasty*, no. 24 (2009): 105-109. https://doi.org/10.1016/j.arth.2009.04.027

10 T. Li, H. Zhang, P.K. Chan et al., "Risk factors associated with surgical site infections following joint replacement surgery: a narrative review," *Arthroplasty*, no. 4 (2026): 11. https://doi.org/10.1186/s42836-022-00113-y

11 I. Lazic, C. Scheele, F. Pohlig et al., "Treatment options in PJI is two-stage still gold standard?," *Journal of Orthopaedics*, no. 23 (2021): 180-184. https://doi.org/10.1016/j.jor.2020.12.021

12 A.D. Martino, G.D. Carlo, D. Pederiva et al., "Which Patients with Chronic Periprosthetic Joint Infection Are Less Suitable to Successful Two Stage Exchange Arthroplasty Surgery? A Retrospective Clinical Trial," *Clinics and Practice*, no. 13 (2023): 190-199. https://doi.org/10.3390/clinpract13010017

13 R.S. Charette and C.M. Melnic, "Two-Stage Revision Arthroplasty for the Treatment of Prosthetic Joint Infection," *Current Reviews in Musculoskeletal Medicine*, no. 11 (2018): 332-340. https://doi.org/10.1007/s12178-018-9495-y

14 P.V. Samelis, E. Papagrigorakis, E. Sameli et al., "Current Concepts on the Application, Pharmacokinetics and Complications of Antibiotic-Loaded Cement Spacers in the Treatment of Prosthetic Joint Infections," *Cureus*, no. 14 (2022): https://doi.org/10.7759/cureus.20968

15 J. Lora-Tamayo, M. Mancheño-Losa, M.Á. Meléndez-Carmona et al., "Appropriate Duration of Antimicrobial Treatment for Prosthetic Joint Infections: A Narrative Review," *Antibiotics*, no. 13 (2024): 293. https://doi.org/10.3390/antibiotics13040293

16 R. Gálvez-López, A. Peña-Monje, R. Antelo-Lorenzo et al., "Elution kinetics, antimicrobial activity, and mechanical properties of 11 different antibiotic loaded acrylic bone cement," *Diagnostic microbiology and infectious disease*, no. 78 (2014): https://doi.org/10.1016/j.diagmicrobio.2013.09.014

17 B. Fink and K.D. Tetsworth, "Antibiotic Elution from Cement Spacers and Its Influencing Factors," *Antibiotics*, no. 14 (2025): 705. https://doi.org/10.3390/antibiotics14070705

18 T. Meng-Lun, H.A. Herng-Shouh, W. Cheng-Ta et al., "Optimal reimplantation timing in two-stage exchange for periprosthetic joint infection: an observative cohort study in Asian population," *BMC Musculoskeletal Disorders*, no. 25 (2024): 28. https://doi.org/10.1186/s12891-023-07129-8

19 P. Jan, H. Marc, G. Georg et al., "Evaluation of time to reimplantation as a risk factor in two-stage revision with static spacers for periprosthetic knee joint infection," *Journal of Orthopaedics and Traumatology*, no. 25 (2024): 1-11. https://doi.org/doi:10.1186/s10195-024-00745-7

20 N.R. Johnson, T.M. Rowe, M.M. Valenzeula et al., "Do Pre-Reimplantation Erythrocyte Sedimentation Rate/C-Reactive Protein Cutoffs Guide Decision-Making in Prosthetic Joint Infection? Are We Flying Blind?," *The Journal of arthroplasty*, no. 37 (2022): https://doi.org/10.1016/j.arth.2021.10.028

21 M. McNally, R. Sousa, M. Wouthuyzen-Bakker et al., "The EBJIS definition of periprosthetic joint infection: a practical guide for clinicians," *The Bone & Joint Journal*, no. 103-B (2021): 18-25. https://doi.org/10.1302/0301-620X.103B1.BJJ-2020-1381.R1

22 L. Drago, P. Clerici, I. Morelli et al., "The World Association against Infection in Orthopaedics and Trauma (WAIOT) procedures for Microbiological Sampling and Processing for Periprosthetic Joint Infections (PJIs) and other Implant-Related Infections," *Journal of Clinical Medicine*, no. 8 (2019): 933. https://doi.org/10.3390/jcm8070933

 doi:10.20944/preprints202604.1875.v1

23 J.A. Mitterer, S.G. Hartmann, S. Simon et al., "Comparison of synovial calprotectin and alpha-defensin for the diagnosis of persistent periprosthetic joint infections at second stage of a two-stage revision arthroplasty," *Archives of orthopaedic and trauma surgery*, no. 145 (2025): 428. https://doi.org/10.1007/s00402-025-06045-x

24 F. Iqbal, B. Shafiq, S.S. Noor et al., "Economic Burden of Periprosthetic Joint Infection Following Primary Total Knee Replacement in a Developing Country," *Clinics in Orthopedic Surgery*, no. 12 (2020): 470-476. https://doi.org/10.4055/cios20037

25 S.M. Kurz, G.B. Higgs, E. Lau et al., "Hospital Costs for Unsuccessful Two-Stage Revisions for Periprosthetic Joint Infection," *osthetic Joint Infection. J Arthroplasty*, no. 37 (2022): 205-212. https://doi.org/doi:10.1016/j.arth.2021.10.018

26 B. Zmistowski, J.A. Karam, J.B. Durinka et al., "Periprosthetic joint infection increases the risk of one-year mortality," *The Journal of bone and joint surgery. American volume*, no. 95 (2013): https://doi.org/10.2106/JBJS.L.00789

27 E.M. Schwarz, J. Parvizi and T. Gehrke, "International Consensus Meeting on Musculoskeletal Infection: Research Priorities from the General Assembly Questions," *J Orthop Res.*, no. 37 (2019): 997-1006. https://doi.org/10.1002/jor.24293

28 C. Li, N. Renz and A. Trampuz, "Management of Periprosthetic Joint Infection," *Hip Pelvis*, no. 30 (2018): 138-146. https://doi.org/10.5371/hp.2018.30.3.138

29 M.R. Hamblin, "Mechanisms and applications of the anti-inflammatory effects of photobiomodulation," *AIMS Biophys.*, no. 4 (2017): 337-361. https://doi.org/10.3934/biophy.2017.3.337

30 D.G. Rathod, H. Muneer and S. Masood. *StatPearls* in *Phototherapy* Treasure Island (FL) (StatPearls Publishing, 2023)

31 L. Gholami, S. Shahabi, M. Jazaeri et al., "Clinical applications of antimicrobial photodynamic therapy in dentistry," *Frontiers in Microbiology*, no. 13 (2023): 1020995. https://doi.org/doi:10.3389/fmicb.2022.1020995

32 P. Woodgate and L.A. Jardine, "Neonatal jaundice: phototherapy," *BMJ Clinical Evidence*, no. 2015 (2015): 0319. https://doi.org/PMID: 25998618

33 M. Mazloumi, L.A. Dalvin, S.-H. Abtahi et al., "Photodynamic Therapy in Ocular Oncology," *Journal of Ophthalmic & Vision Research*, no. 15 (2020): 547. https://doi.org/10.18502/jovr.v15i4.7793

34 W. Jiang, M. Liang, Q. Lei et al., "The Current Status of Photodynamic Therapy in Cancer Treatment," *Cancers*, no. 15 (2023): 585. https://doi.org/10.3390/cancers15030585

35 Y. Liu, R. Qin, S.A.J. Zaat et al., "Antibacterial photodynamic therapy: overview of a promising approach to fight antibiotic-resistant bacterial infections," *Journal of Clinical and Translational Research*, no. 1 (2015): 140-167. https://doi.org/DOI: 10.18053/jctres.201503.002

36 Y. Wang, Y. Wang, Y. Wang et al., "Antimicrobial blue light inactivation of pathogenic microbes: state of the art," *Drug resistance updates*, no. 33-35 (2017): 1-22. https://doi.org/doi:10.1016/j.drup.2017.10.002

37 *BoneSens-Our Progress*, <https://bonesens.com/Our-Progress>.(Access date: 28.11.2025)

38 C. Dillitzer, N.B. Tran, P. Morandell et al. in *International Conference on Engineering for Life Sciences: ENROL 2025*.

39 C. Dillitzer, N.B. Tran and O. Hayden. *Scattering spectra acquisition and algorithmic analysis to distinguish between different bacterial concentrations of Staphylococcus Aureus as an application of a SmartSpacer system for two-stage knee total endoprosthesis (KTEP) revision*. Vol. PC12837, San Francisco, SPIE,

40 N.B. Tran, V. Bub and C. Dillitzer. *Discrimination of bacterial concentrations of Staphylococcus Aureus based on statistical spectral analysis using a smart-spacer prototype with a low-resolution spectrometer unit as an application during two-stage total endoprosthesis (TEP) revision*. Vol. 12387, SPIE,

41 T. German Federal Ministry of Education and Research (BMBF) since 2025 Federal Ministry of Research, and Space (BMFTR). "SWi2M; Intelligentes drahtloses Implantat zur Infektionsüberwachung - Entwicklung eines miniaturisierten Sensorsystems," Report No. FKZ: 01EK2107A, (BMBF now BMFTR, 2022), https://bonesens.com/, (Access date: 20.04.2026).

42 H.K. Walker and V.E. Del-Bene. in *Clinical Methods: The History, Physical, and Laboratory Examinations* Ch. 218, (Butterworths, 1990).https://www.ncbi.nlm.nih.gov/pubmed/, (Access date: 20.04.2026)

 doi:10.20944/preprints202604.1875.v1

43 S. Zhang, P. Li, X. Xu et al., "No-Reference Image Blur Assessment Based on Response Function of Singular Values," *Symmetry*, no. 10 (2018): 304. https://doi.org/10.3390/sym10080304

44 L. Glänzer, H.E. Masalkhi, A.A. Roeth et al., "Vessel Delineation Using U-Net: A Sparse Labeled Deep Learning Approach for Semantic Segmentation of Histological Images," *Cancers*, no. 15 (2023): 3773. https://doi.org/10.3390/cancers15153773

45 X. Chen, Q. Zhang and M. Lin, "No-Reference Color Image Quality Assessment: From Entropy to Perceptual Quality," *EURASIP Journal on Image and Video Processing*, no. 77 (2019): 2019. https://doi.org/doi.org/10.1186/s13640-019-0479-7

46 F. Krauß, "BlaVeS: Bladder Vessel Segmentation," v 1 (2025). https://doi.org/doi:10.18419/DARUS-4763

47 I.D.C. Galo, R.P. Prado and W.G.D. Santos, "Blue and red light photoemitters as approach to inhibit Staphylococcus aureus and Pseudomonas aeruginosa growth," *Brazilian journal of biology*, no. 82 (2021): https://doi.org/10.1590/1519-6984.231742

48 I.D.C. Galo, B.E. Lima, T.G. Santos et al., "Staphylococcus aureus growth delay after exposure to low fluencies of blue light (470 nm)," *Brazilian journal of biology*, no. 81 (2021): https://doi.org/10.1590/1519-6984.226473

49 T. Dai, C.K. Murray, M.S. Vrahas et al., "Ultraviolet C light for Acinetobacter baumannii wound infections in mice: potential use for battlefield wound decontamination?," *The journal of trauma and acute care surgery*, no. 73 (2012): 661-667. https://doi.org/10.1097/TA.0b013e31825c149c

50 J.W. Costerton, P.S. Stewart and E.P. Greenberg, "Bacterial biofilms: a common cause of persistent infections," *Science (New York, N.Y.)*, no. 284 (1999): 1318-1322. https://doi.org/10.1126/science.284.5418.1318

51 M.R. Hamblin and T. Hasan, "Photodynamic therapy: a new antimicrobial approach to infectious disease?," *Photochemical & photobiological sciences : Official journal of the European Photochemistry Association and the European Society for Photobiology*, no. 3 (2004): 436-450. https://doi.org/10.1039/b311900a

52 Y. Ou and P.M. Petersen, "Application of ultraviolet light sources for in vivo disinfection - IOPscience," *Japanese Journal of Applied Physics*, (2021): 100501. https://doi.org/doi:10.35848/1347-4065/ac1f47

53 International Commission on Radiological Protection. "The 2007 Recommendations of the International Commission on Radiological Protection. ICRP publication 103," Report No. 0146-6453, (ICRP, 2007), https://www.ncbi.nlm.nih.gov/pubmed/18082557, (Access date:

54 E. Union. "Directive 2013/59/Euratom - protection against ionising radiation," (2013), https://osha.europa.eu/en/legislation/directives/directive-2013-59-euratom-protection-against-ionising-radiation, (Access date: 20.04.2026).

55 I.E. Commission. "IEC 60601-1-2: Medical electrical equipment – Part 1-2: General requirements for basic safety and essential performance – Collateral standard: Electromagnetic disturbances – Requirements and tests," Report No. IEC 60601-1-2, (International Electrotechnical Commission, 2014), https://www.vde-verlag.de/iec-normen/249094/iec-60601-1-2-2014-amd1-2020-csv.html, (Access date: 19.04.2026).

56 I.E. Commission. "IEC 60601-2-33: Medical electrical equipment – Part 2-33: Particular requirements for the basic safety and essential performance of magnetic resonance equipment for medical diagnosis," (International Electrotechnical Commission, 2015), https://www.vde-verlag.de/iec-normen/251063/iec-60601-2-33-2022.html, (Access date: 19.04.2026).

57 S. Yokomizo, M. Roessing, A. Morita et al., "Near-infrared II photobiomodulation augments nitric oxide bioavailability via phosphorylation of endothelial nitric oxide synthase," *FASEB journal*, no. 36 (2022): https://doi.org/10.1096/fj.202101890R

58 J. Cadet and T. Douki, "Formation of UV-induced DNA damage contributing to skin cancer development," *Photochemical & photobiological sciences*, no. 17 (2018): 1816-1841. https://doi.org/10.1039/c7pp00395a

59 W. Kowalski. *Ultraviolet Germicidal Irradiation Handbook: UVGI for Air and Surface Disinfection*. Berlin / Heidelberg, Springer, ISBN 978-3-642-01998-2.

60 F.R.d. Gruijl, "Photocarcinogenesis: UVA vs UVB," *Methods in enzymology*, no. 319 (2000): https://doi.org/10.1016/s0076-6879(00)19035-4

61 K. Ishida, M. Matsubara, M. Nagahashi et al., "Efficacy of ultraviolet-light emitting diodes in bacterial inactivation and DNA damage via sensitivity evaluation using multiple wavelengths and bacterial strains," *Archives of Microbiology*, no. 207 (2025): 130. https://doi.org/10.1007/s00203-025-04324-0

 doi:10.20944/preprints202604.1875.v1

62 P. Montero, I. Roger, J. Milara et al., "Damaging effects of UVA, blue light, and infrared radiation: in vitro assessment on a reconstructed full-thickness human skin," *Frontiers in Medicine*, no. 10 (2023): 1267409. https://doi.org/10.3389/fmed.2023.1267409

63 H. Chen, Y. Cheng and C.I. Moraru, "Blue 405 nm LED light effectively inactivates bacterial pathogens on substrates and packaging materials used in food processing," *Scientific Reports*, no. 13 (2023): 15472. https://doi.org/10.1038/s41598-023-42347-z

64 R. Tamimi, N.M. Mahmoodi, H.R. Samadikhah et al., "Anti-inflammatory effect of green photobiomodulation in human adipose-derived mesenchymal stem cells," *Lasers in Medical Science*, no. 37 (2022): 3693-3703. https://doi.org/10.1007/s10103-022-03654-5

65 Y.T. Kang, T.T. Tri, D.S. Jo et al., "Impact of Red and Red/NIR OLEDs photobiomodulation effects towards promoting ADMSCs chondrogenic differentiation," *Tissue and Cell*, no. 96 (2025): 102948. https://doi.org/10.1016/j.tice.2025.102948

66 G.B. Kharkwal, S.K. Sharma, Y.-Y. Huang et al., "Photodynamic Therapy for Infections: Clinical Applications," *Lasers in surgery and medicine*, no. 43 (2011): 755. https://doi.org/10.1002/lsm.21080

67 H. Chung, T. Dai, S.K. Sharma et al., "The nuts and bolts of low-level laser (light) therapy," *Annals of biomedical engineering*, no. 40 (2012): https://doi.org/10.1007/s10439-011-0454-7

68 L.M. Ailioaie and G. Litscher, "Probiotics, Photobiomodulation, and Disease Management: Controversies and Challenges," *International Journal of Molecular Sciences*, no. 22 (2021): 4942. https://doi.org/10.3390/ijms22094942

69 T.I. Karu, "Mitochondrial signaling in mammalian cells activated by red and near-IR radiation," *Photochemistry and photobiology*, no. 84 (2008): 1091-1099. https://doi.org/10.1111/j.1751-1097.2008.00394.x

70 P.V.d. Silveira, B.H.D. Panariello, C.A.G.d. Araújo-Costa et al., "Twice-daily red and blue light treatment for Candida albicans biofilm matrix development control," *Lasers in medical science*, no. 34 (2019): 441-447. https://doi.org/10.1007/s10103-018-2610-x

71 C. Wang, Z. Yang, Y. Peng et al., "Application of 460 nm visible light for the elimination of Candida albicans in vitro and in vivo," *Molecular medicine reports*, no. 18 (2018): 2017-2026. https://doi.org/10.3892/mmr.2018.9196

72 K. Makdoumi, M. Hedin and A. Bäckman, "Different photodynamic effects of blue light with and without riboflavin on methicillin-resistant Staphylococcus aureus (MRSA) and human keratinocytes in vitro," *Lasers in medical science*, no. 34 (2019): 1799-1805. https://doi.org/10.1007/s10103-019-02774-9

73 K. Makdoumi, R. Goodrich and A. Bäckman, "Photochemical eradication of methicillin-resistant Staphylococcus aureus by blue light activation of riboflavin," *Acta ophthalmologica*, no. 95 (2017): 498-502. https://doi.org/10.1111/aos.13409

74 R. Bauer, K. Hoenes, T. Meurle et al., "The effects of violet and blue light irradiation on ESKAPE pathogens and human cells in presence of cell culture media," *Scientific reports*, no. 11 (2021): 24473. https://doi.org/10.1038/s41598-021-04202-x

75 W.A. Rutala, H. Kanamori, M.F. Gergen et al., "Antimicrobial activity of a continuous visible light disinfection system," *Infection control and hospital epidemiology*, no. 39 (2018): 1250-1253. https://doi.org/10.1017/ice.2018.200

76 M. Maclean, J.G. Anderson, S.J. MacGregor et al., "A New Proof of Concept in Bacterial Reduction: Antimicrobial Action of Violet-Blue Light (405 nm) in Ex Vivo Stored Plasma," *Journal of blood transfusion*, no. 2016 (2016): 2920514. https://doi.org/10.1155/2016/2920514

77 M. Maclean, K. McKenzie, J.G. Anderson et al., "405 nm light technology for the inactivation of pathogens and its potential role for environmental disinfection and infection control," *The Journal of hospital infection*, no. 88 (2014): 1-11. https://doi.org/10.1016/j.jhin.2014.06.004

78 M. Maclean, S.J. MacGregor, J.G. Anderson et al., "High-intensity narrow-spectrum light inactivation and wavelength sensitivity of Staphylococcus aureus," *FEMS microbiology letters*, no. 285 (2008): 227-232. https://doi.org/10.1111/j.1574-6968.2008.01233.x

79 R.M. Tomb, T.A. White, J.E. Coia et al., "Review of the Comparative Susceptibility of Microbial Species to Photoinactivation Using 380-480 nm Violet-Blue Light," *Photochemistry and photobiology*, no. 94 (2018): 445-458. https://doi.org/10.1111/php.12883

 doi:10.20944/preprints202604.1875.v1

80 C.S. Enwemeka, T.L. Baker and V.V. Bumah, "The role of UV and blue light in photo-eradication of microorganisms," *Journal of Photochemistry and Photobiology*, no. 8 (2021): 100064. https://doi.org/10.1016/j.jpap.2021.100064

81 P.P. Rullan, "A Handheld Broadband UV Phototherapy Module for the Treatment of Patients With Psoriasis and Vitiligo," *Cutis*, no. 86 (2010): 321–326.

82 M. Robatto, M.C. Pavie, I. Garcia et al., "Ultraviolet A/blue light-emitting diode therapy for vulvovaginal candidiasis: a case presentation," *Lasers in Medical Science*, no. 34 (2019): 1819-1827. https://doi.org/doi:10.1007/s10103-019-02782-9

83 A. Rezaie, G.G.S. Leite, G.Y. Melmed et al., "Ultraviolet A light effectively reduces bacteria and viruses including coronavirus," *PLOS ONE*, no. 15 (2020): e0236199. https://doi.org/10.1371/journal.pone.0236199

84 A. Rezaie, G.Y. Melmed, G. Leite et al., "Endotracheal Application of Ultraviolet A Light in Critically Ill Patients with Severe Acute Respiratory Syndrome Coronavirus 2: A First-in-Human Study," *Advances in Therapy*, no. 38 (2021): 4556-4568. https://doi.org/doi:10.1007/s12325-021-01830-7

85 R.R. Anderson and J.A. Parrish, "The optics of human skin," *The Journal of investigative dermatology*, no. 77 (1981): 13-19. https://doi.org/10.1111/1523-1747.ep12479191

86 R. Gläser, F. Navid, W. Schuller et al., "UV-B radiation induces the expression of antimicrobial peptides in human keratinocytes in vitro and in vivo," *Journal of Allergy and Clinical Immunology*, no. 123 (2009): 1117-1123. https://doi.org/10.1016/j.jaci.2009.01.043

87 L. Mallbris, D.W. Edström, L. Sundblad et al., "UVB Upregulates the Antimicrobial Protein hCAP18 mRNA in Human Skin," *Journal of Investigative Dermatology*, no. 125 (2005): 1072-1074. https://doi.org/10.1111/j.0022-202X.2005.23872.x

88 S.P. Hong, M.J. Kim, M. Jung et al., "Biopositive Effects of Low-Dose UVB on Epidermis: Coordinate Upregulation of Antimicrobial Peptides and Permeability Barrier Reinforcement," *Journal of Investigative Dermatology*, no. 128 (2008): 2880-2887. https://doi.org/10.1038/jid.2008.169

89 T. Gambichler, R.U.o.B. Department of Dermatology, Gudrunstr. 56, D-44791 Bochum, Germany, M. Skrygan et al., "Changes of antimicrobial peptide mRNA expression in atopic eczema following phototherapy," *British Journal of Dermatology*, no. 155 (2024): 1275-1278. https://doi.org/10.1111/j.1365-2133.2006.07481.x

90 K. Vähävihu, M. Ala-Houhala, M. Peric et al., "Narrowband ultraviolet B treatment improves vitamin D balance and alters antimicrobial peptide expression in skin lesions of psoriasis and atopic dermatitis," *The British journal of dermatology*, no. 163 (2010): 321-328. https://doi.org/10.1111/j.1365-2133.2010.09767.x

91 L.K. Dotterud, T. Wilsgaard, L.H. Vorland et al., "The effect of UVB radiation on skin microbiota in patients with atopic dermatitis and healthy controls," *International journal of circumpolar health*, no. 67 (2008): 254-260. https://doi.org/10.3402/ijch.v67i2-3.18282

92 S. Silva, A. Guedes, B. Gontijo et al., "Influence of narrow-band UVB phototherapy on cutaneous microbiota of children with atopic dermatitis," *Journal of the European Academy of Dermatology and Venereology*, no. 20 (2006): 1114-1120. https://doi.org/https://doi.org/10.1111/j.1468-3083.2006.01748.x

93 H. Shimoda, J. Matsuda, T. Iwasaki et al., "Efficacy of 265-nm ultraviolet light in inactivating infectious SARS-CoV-2," *Journal of photochemistry and photobiology*, no. 7 (2021): 100050. https://doi.org/10.1016/j.jpap.2021.100050

94 M. Buonanno, M. Stanislauskas, B. Ponnaiya et al., "207-nm UV Light—A Promising Tool for Safe Low-Cost Reduction of Surgical Site Infections. II: In-Vivo Safety Studies," *PLOS ONE*, no. 11 (2016): e0138418. https://doi.org/10.1371/journal.pone.0138418

95 T. Dai, G.B. Kharkwal, J. Zhao et al., "Ultraviolet-C Light for Treatment of Candida albicans Burn Infection in Mice," *Photochemistry and Photobiology*, no. 87 (2011): 342-349. https://doi.org/https://doi.org/10.1111/j.1751-1097.2011.00886.x

96 T. Dai, B. Garcia, C.K. Murray et al., "UVC Light Prophylaxis for Cutaneous Wound Infections in Mice," *Antimicrob Agents Chemother*, (2012): https://doi.org/10.1128/aac.00161-12

97 T.P. Thai, P.E. Houghton, K.E. Campbell et al., "Ultraviolet light C in the treatment of chronic wounds with MRSA: a case study," *Ostomy/wound management*, no. 48 (2002): 52-60.

 doi:10.20944/preprints202604.1875.v1

98 B. Ponnaiya, M. Buonanno, D. Welch et al., "Far-UVC light prevents MRSA infection of superficial wounds in vivo | PLOS ONE," *PLOS ONE*, no. 13 (2018): e0192053. https://doi.org/10.1371/journal.pone.0192053

99 J. Glaab, N. Lobo-Ploch, H.K. Cho et al., "Skin tolerant inactivation of multiresistant pathogens using far-UVC LEDs," *Scientific Reports*, no. 11 (2021): 1-11. https://doi.org/doi:10.1038/s41598-021-94070-2

100 P. Zwicker, J. Schleusener, S.B. Lohan et al., "Application of 233 nm far-UVC LEDs for eradication of MRSA and MSSA and risk assessment on skin models," *Scientific Reports*, no. 12 (2022): 1-15. https://doi.org/doi:10.1038/s41598-022-06397-z

101 J. Schleusener, S.B. Lohan, L. Busch et al., "Irradiation of human oral mucosa by 233 nm far UV-C LEDs for the safe inactivation of nosocomial pathogens," *Scientific Reports*, no. 13 (2023): 1-12. https://doi.org/doi:10.1038/s41598-023-49745-3

102 K. Narita, K. Asano, Y. Morimoto et al., "Disinfection and healing effects of 222-nm UVC light on methicillin-resistant Staphylococcus aureus infection in mouse wounds," *Journal of Photochemistry and Photobiology B: Biology*, no. 178 (2018): 10-18. https://doi.org/https://doi.org/10.1016/j.jphotobiol.2017.10.030

103 T. Fukui, T. Niikura, T. Oda et al., "Exploratory clinical trial on the safety and bactericidal effect of 222-nm ultraviolet C irradiation in healthy humans," *PLOS ONE*, no. 15 (2020): e0235948. https://doi.org/10.1371/journal.pone.0235948

104 M. Buonanno, B. Ponnaiya, D. Welch et al., "Germicidal Efficacy and Mammalian Skin Safety of 222-nm UV Light," *Radiation Research*, no. 187 (2017): 493-501. https://doi.org/10.1667/RR0010CC.1